91602
new 82-10

COMPLIMENTARY COPY
Please Credit Ontario Hydro Research if Reproduced in Whole or in Part.

ontario hydro research division

ULTRASONIC INSPECTION OF CANDIDATE USED FUEL CONTAINER WELD MATERIALS

Report No 84-227-K

M.D.C. Moles and J. Imada
Nondestructive and Fracture Evaluation Section
Metallurgical Research Dept

ABSTRACT

Ultrasonic inspections have been performed on welds of candidate materials for used fuel container materials (copper, titanium grades 2 and 12, stainless steel 316, Inconel 625 and Hastelloy C-276) to determine ultrasonic anisotropy, in particular beam skewing. The results showed that the titanium welds were essentially isotropic. However, the other weld metals all showed significant anisotropy and problems with inspection of final closure welds can be anticipated with these materials.

job	file	date	report no.
740683-326-461	826.14	August 22, 1984	84-227-K

91602
new 82-10

ontario hydro
research division

EXECUTIVE SUMMARY

ULTRASONIC INSPECTION OF CANDIDATE USED FUEL CONTAINER WELD MATERIALS

M.D.C. Moles and J. Imada
Nondestructive & Fracture Evaluation Section
Metallurgical Research Department

Ultrasonic inspection of weld cylinders of candidate used fuel container materials (copper, titanium grades 2 and 12, stainless steel 316, Inconel 625, Hastelloy C-276) using immersion longitudinal waves showed that titanium grades 2 and 12 exhibited essentially isotropic behaviour (little beam skewing). The other materials all showed significant anisotropy, which will probably present inspection problems for final closure welds, though there are a number of techniques available for reducing these problems. These include spatial signal averaging, appropriate ultrasonic inspection procedures, multiple beam inspection techniques and grain refinement. Metallography showed that the stainless steel, Inconel and Hastelloy all had long columnar grains, but that the copper showed columnar grains round each weld pass with equiaxed grains in the centres. Altering weld interpass temperatures produced no consistent trend in ultrasonic behaviour.

Recommendations include performing beam skewing measurements on these welds using shear waves, and performing ultrasound coupling studies using waterjets rather than full immersion.

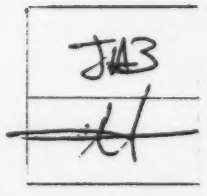

job	file	date	report no.
740683-326-461	826.14	August 22, 1984	84-227-K

TABLE OF CONTENTS

		Page
1.0	INTRODUCTION	1
	1.1 Background	1
	1.2 Previous Work	2
2.0	EXPERIMENTAL PROCEDURE	4
	2.1 Cylinder Preparation	4
	2.2 Scanning Procedures	4
	2.3 Numerical Analysis Procedures	5
	2.3.1 Plot Width	5
	2.3.2 Skew Angle	6
	2.3.3 Number of Peaks	6
	2.3.4 Comments on Numerical Analysis	6
3.0	RESULTS	7
	3.1 Metallography	7
	3.2 Ultrasonic Scan Results	8
	3.3 Analysis of Results	8
4.0	DISCUSSION	9
	4.1 General Comments	9
	4.2 Future Work Areas	9
5.0	CONCLUSIONS	10
6.0	RECOMMENDATIONS	11
	ACKNOWLEDGEMENTS	11
	REFERENCES	12
	TABLES	14
	FIGURES	17

LIST OF TABLES

TABLE 1 - Welds Prepared

TABLE 2 - Summary of Measurements for Each Cylinder

TABLE 3 - Cylinder Ranking

LIST OF FIGURES

FIGURE 1 - Weld Layout

FIGURE 2 - Equipment Set-Up

FIGURE 3 - The Three Individual Scan Measurements

a) Plot Width, b) Skew Angle, c) Number of Peaks

FIGURE 4 - Microstructures of the Candidate Weld Materials (from the ends of the cylinders)

a) stainless steel X5	b) stainless steel X20
c) titanium grade 2 X5	d) titanium grade 2 X20
e) titanium grade 12 LT X5	f) titanium grade 12 LT X20
g) titanium grade 12 HT X5	h) titanium grade 12 HT X20
i) copper LT X5	j) copper LT X20
k) copper HT X5	l) copper HT X20
m) Inconel 625 LT X5	n) Inconel 625 LT X20
o) Inconel 625 HT X5	p) Inconel 625 HT X20
r) Hastelloy C-276 LT X5	s) Hastelloy C-276 LT X20
t) Hastelloy C-276 HT X5	u) Hastelloy C-276 HT X20

FIGURE 5 - Sample Plots Generated from Scans

FIGURE 6 - Isometric Display of Scan Plots

a) mild steel rod	b) mild steel weld
c) stainless steel 316	d) titanium grade 2
e) titanium grade 12 LT	f) titanium grade 12 HT
g) copper LT	h) copper HT
i) Inconel 625 LT	j) Inconel 625 HT
k) Hastelloy C-276 LT	l) Hastelloy C-276 HT

FIGURE 7 - Reference Notation for Plots (after/19/)

FIGURE 8 - Variation of Skew Angle with Cylinder Orientation

a) mild steel rod	b) mild steel weld
c) stainless steel	d) titanium grade 2
e) titanium grade 12 LT	f) titanium grade 12 HT
g) copper LT	h) copper HT
i) Inconel 625 LT	j) Inconel 625 HT
k) Hastelloy C-276 LT	l) Hastelloy C-276 HT

ontario hydro
research division

To
Mr. H.N. Isaac
Manager
Nuclear Materials Management
H10A27

ULTRASONIC INSPECTION OF CANDIDATE
USED FUEL CONTAINER WELD MATERIALS

1.0 INTRODUCTION

1.1 Background

As irradiated used fuel from CANDU nuclear reactors continues to be produced, it has become necessary to investigate methods for its long-term disposal. One such proposal involves the placement of containers filled with waste fuel underground in a stable rock vault. The container must be non-corrosive, impermeable, and capable of withstanding high temperatures and pressures to ensure that during its design life of 500 years, the contents are isolated from the environment/1/.

Although several designs are under consideration, most containers consist of a metal cylindrical body and a lid. A weld between these two parts is required in order to seal the container, which must be perfo-rmed remotely due to high radiation fields. Inspection is then necessary to verify that the weld does not contribute any potential areas of leakage or mechanical weakness to the container. Ultrasonics has been established as the most viable method of volumetric inspection. However, difficulties in inspecting welds ultrasonically have been encountered with some of the candidate container materials due to substantial beam scattering and attenuation (see Section 1.2 below). This behaviour has been related to the formation of large grains in welds with a preferred orientation, producing an acoustically anisotropic microstructure.

As part of the Canadian Container Development Program for Fuel Isolation/2/, a number of materials have been selected as possible candidates for used fuel containers, primarily on the strength of their corrosion resistance. These materials are:

1. 316L stainless steel
2. Titanium grade 2
3. Titanium grade 12
4. Commercially pure copper
5. Inconel 625
6. Hastelloy C-276

Welds of these materials, plus a mild steel weld and rod, were manufactured and examined ultrasonically to determine anisotropy (see section 2.2). Since smaller grain sizes are generally considered more beneficial than large sizes, two welds of each material (except 316 stainless and titanium grade 2) were manufactured, one at a high interpass temperature, the other at a lower interpass temperature to inhibit grain growth.

In contrast to other workers/3-20/, who have been primarily interested in either characterizing or improving inspectability of materials, the objective of this work was to rank the various materials in terms of their ultrasonic inspectability. Consequently, numerical/statistical analysis have been developed and performed on the data generated.

1.2 Previous Work

A considerable amount of work has been performed by other workers on characterizing the ultrasonic behaviour of austenitic-type welds from several different aspects/3-19/. Most of the work has been performed on 300 series stainless steels, with the balance on Inconel 82, which is also used for reactor vessel cladding. This work has ranged from theoretical and experimental analysis to modelling beam skewing to developing techniques for improving inspectability.

Kupperman et al/8-10,17/, Tomlinson et al/19/. and Adler et al/4,6/ have shown that austenitic welds typically consist of large grains growing wih their <001> direction in the z-plane (see figure 1), with fairly random x and y orientations. In contrast to ferritic steels, no phase transformations occur in austenitic steels on cooling, so no recrystallization, and hence randomization, of the microstructure occurs. Thus, the austenitic-type weld microstructures consist of very long, oriented grains in the z (out of weld plane) direction. This can have three effects/9/: (1) ultrasonic attenuation increases due to grain boundary scattering, though this would not be a major problem for thin-walled containers; (2) mode conversions can occur; and (3), most important for nuclear waste containers, beam steering skewing occurs because ultrasonic beams are diffracted by changes in velocity between grains of different orientations.

Crystallographic-type studies/4,6,8-10,17,19/ have shown that ultrasonic velocity (and hence beam skewing) can be fairly satisfactorily correlated with single-crystal elastic constants and with resulting theoretical models, given the expected variation between welds. Kupperman et al in particular/10/ have shown that longitudinal waves can expect a beam skewing of up to 21° at certain orientations in stainless steels, while shear waves polarized in the vertical direction (SV) can undergo skewing up to 44°, and SH waves (horizontally polarized shear waves) up to 13°. Longitudinal waves are least affected at a 45° refracted angle (relative to the z-axis), while SV waves are worst at around 45° to 60° refracted angles/6,9/. Unfortunately, most ultrasonic inspections use 45°-60° angles with shear waves, since for many welds the weld z-axis is perpendicular to the inspection surface.

A beam skewing model has been developed by Silk/4/, using a finite element-type mesh to model the changes in velocity and other physical properties in anisotropic welds. Kupperman et al/10/ have developed a model for predicting beam skewing, which correlates reasonably with experimental results.

Other workers have attempted to improve inspectability by signal processing or other means. Mech et al/5/ and Dau/3/ have investigated adaptive learning techniques for improving characterization of defects, with some success. Murali and Neelakantan/15/ have developed a manual spatial signal-averaging technique to improve signal-to-noise ratio, while Kupperman et al/11/ have developed a special purpose computer-controlled jig for a similar purpose. Spatial signal averaging techniques are likely to be particularly applicable to large grained, and hence "noisy" microstructures. Alternatively, a number of workers have pointed out that fine-grained welds typically should be more easily inspected than coarse-grained welds/9,18/.

Caussin et al/12/ have shown experimentally that results vary considerably with welding technique and with the individual welds. In contrast, Edelmann/13/ recommends extensive use of reference blocks to establish reproducible standards. Singh/20/, inspecting extruded pipes with side-drilled holes which also showed ultrasonic anisotropy, has developed a double inspection technique to compensate for expected variations in ultrasonic properties. The first inspection uses shear-waves in pitch-catch, essentially to characterize the material, while the second inspection uses longitudinal waves in pulse-echo to characterize defects. Heinrich et al/16/ recommend the use of specific equipment such as 70° longitudinal wave twin probes. Lott and Malik/18/ have shown that hot-isostatic pressing significantly randomizes microstucture and other benefits and hence improves inspectability, whereas heat treatment has little effect.

2.0 EXPERIMENTAL PROCEDURE

Cylinders composed entirely of weld metal were prepared from weld plates of candidate container materials. Ultrasonic scans were then performed by focussing the transmitting probe on the cylinder and rotating the receiving probe around it. By monitoring the ultrasound exiting from the cylinder, skewing and scattering of the ultrasonic beam were determined. Scans were done for several orientations of each cylinder.

2.1 Cylinder Preparation

Welds were prepared from the following materials:

1. Mild Steel
2. 316L Stainless Steel
3. Titanium Grade 2
4. Titanium Grade 12
5. Copper
6. Inconel 625
7. Hastelloy C-276

Thick-section GTA welds were made following standard welding procedures for all the materials, with the exception of interpass temperature. All welds had butt joints and single V-grooves with the final plate dimensions of 15 cm square and 25.4 mm thick (Figure 1). The parent plate and filler metal were the same material in all cases. Table 1 lists each weld with the interpass temperatures and number of passes applied. In order to distinguish between welds of similar material, "LT" refers to the weld with the lower interpass temperatures and "HT" refers to the higher temperature.

Cylinders with a 19.1 mm diameter and length of approximately 76 mm were then machined from each weld (Figure 1). In addition, a block with dimensions 12.7 x 19.1 x 25.4 mm, was cut in order to make attenuation and velocity measurements (not covered in this report).

One end of each cylinder was then polished and etched to examine the microstructure and to establish the direction of the weld passes. A mild steel cylinder not composed of weld metal was also prepared for use as reference material.

2.2 Scanning Procedures

A test procedure used by Tomlinson et al/19/ was followed. Equipment was set up as shown in Figure 2. In each scan, the turntable holding the cylinder and transmitting probe, was rotated 180 degrees while the receiver remained stationary. The transmitter and receiver were in

line after 90 degrees of rotation, and the height of both probes during all scans was the same. Thirty-six scans in total were taken from each cylinder. For the initial scan, the cylinder was oriented such that the transmitting probe faced the base (root pass region) of the weld, arbitrarily called 0 degrees. In the scans which followed, the cylinder was rotated counterclockwise in 10 degree intervals. All scans involved longitudinal ultrasonic waves, not shear waves as with most ultrasonic inspections (though in general the longitudinal and shear wave behaviour of welds will be related).

Daily checks were done to ensure that the setup remained fairly consistent throughout the scans. (Also, moving the cylinder up or down in the holder had surprisingly little effect on the reproducibility of the results). The equipment used consisted of an Apple II Plus computer, stepping motor driver, rotating turntable, water tank, probe holders, immersion probes and a Krautkramer USIP 11 ultrasonic instrument with analog output. Probes were selected after using the ray-tracing program UT PATH to determine suitable focal lengths and waterpaths for the cylinders. In practice, a broadband 25 MHz Aerotech Alpha probe, 50 mm focal length and 6.3 mm diameter was chosen as the pulser, and a 50 mm, 6.3 mm diameter 10 MHz Aerotech Alpha as the receiver after experimentation with the mild steel rod. The USIP 11 was set at 2-8 MHz frequency, so the signals in this range were primarily amplified. Frequencies of 2-8 MHz are typical for inspections. Water path was set at 34 mm.

Strictly speaking, there was not a perfect correlation between the signal amplitudes measured on the USIP 11 CRT screen and from its analog output. It was found that the USIP 11's analog output was primarily a measure of the amplitude of the halfwave negative signal. In practice, this was only detectable on the highly anisotropic welds, and is probably of little practical significance.

2.3. Numerical Analysis Procedures

From each scan, three measurements were taken as a basis to assess and compare the weld materials.

2.3.1 Plot Width

The width of the plot 6 dB below the maximum signal amplitude was measured. This distance, with units in degrees of rotation, was taken from the first signal encountered at this level to the last, all inclusive (Figure 3a). These values give a measure of the extent the beam is scattered in the weld.

2.3.2 Skew Angle

The angle of rotation of the highest peak from the 90 degree mark (straight through, no skewing) was measured. If the peak was situated 0 to 90 degres into the scan, the angle of skew was considered negative, and from 90 to 180 degrees, positive (Figure 3b). For a well-behaved material, the skew angle should be 0 degrees. If more than one peak with the maximum signal was encountered in a single scan, the skew angle was taken from the peak which appeared to have a wider base. Mean and standard deviations were calculated.

2.3.3 Number of Peaks

The number of peaks on each plot was counted. Peaks were classified as being either major or minor. A major peak defined a part of the scan where definite beam skew was occurring. A minor peak accounted for smaller peaks on the scans where it was evident that beam energy was being directed deliberately, rather than in a random manner. The following, essentially arbitrary, criteria were used to define a peak:

a) All peaks must be at or above the level 6 dB down from the maximum signal.

b) There must be at least one half of the 0 to 6 dB height between two major peaks.

c) Minor peaks must have either a base width of at least 10 degrees of rotation, or a height greater than or equal to one tenth the 0 to 6 dB distance.

Peak heights were measured from the higher of the two points dividing a peak from its neighbouring peaks (Figure 3c).

2.3.4 Comments On Numerical Analyses

These analysis procedures were an attempt to assess the results in a simple, fairly objective manner. The 6 dB width is probably a reasonable assessment of spread, though the figures must be interpreted with care. For example, going from 50^{o} mean width to 75^{o} may be a 50% increase, but in practice it means going from a low beam spread material to a high beam spread material.

For beam skew, the average value may not be meaningful if the values average around zero (see section 3). The standard deviation, which is the commonest measure of spread in a distribution, is more meaningful, but fails to take into account any trends within the data. Since trends with orientation were observed by Kupperman et al/9/, results are given in both isometric plots and tabular form so trends can be

observed. Despite this shortcoming, for this study the standard deviation of the beam skew is probably the single most important parameter.

The number of peaks, both minor and major, is not based on any scientific rationale, but is an attempt to numerically assess an obvious visual phenomenon.

3.0 RESULTS

3.1 Metallography

Micrographs of the etched weld cylinders are shown in figures 4a - 4u at low magnification (x5) and medium magnification (x20). The weld passes were clearly visible for identifying the z-axis, except for the titanium grade 2 despite several etching attempts. (Since the z-axis for this weld could not be identified, an initial orientation was chosen arbitrarily. This was not important since the material proved highly isotropic).

Figures 4a and 4b show the microstructure of the stainless steel weld cylinder. Elongated grains are very visible in both figures, approaching 1 mm in length. Figures 4c and 4d show the titanium grade 2 microstructure, where very extensive recrystallizatin has occurred, resulting in a fine-grained, equiaxed structure. Figures 4e and 4f show the Ti grade 12 LT weld with the weld passes and elongated grains in the z-axis visible. Some internal transformations are visible within the larger grains in Figure 4f. Similar comments can be made about the titanium grade 12 HT weld (figures 4g and 4h), where even longer grains are visible (compare figures 4e and 4g).

Figures 4i and 4j show the copper LT weld. The microstructure consists of relatively large equiaxed grains in the centre of each weld pass with columnar grains oriented onwards. This is typical of a cast structure and is consistent with the very high heat transfer rates of copper. Figures 4k and 4l show the HT copper weld, and similar comments can be made about the grain structure.

Figures 4m and 4n show the LT Inconel 625 weld. The weld passes are clearly visible, as well as elongated grains, though these appear smaller than the stainless steel grains. Figures 4o and 4p show the HT Inconel weld. Figures 4s and 4r show the LT Hastelloy weld, which shows long columnar grains, though not as long as the stainless steel. Figures 4t and 4u, HT Hastelloy weld, are similar to figures 4r and 4s.

3.2 Ultrasonic Scan Results

Directly from each ultrasonic scan, a plot was generated showing the distribution of signal strength transmitted around the cylinder. Two examples of individual plots (one isotropic, one anisotropic) are shown in Figure 5. Plots for each cylinder were assembled in an isometric plot (Figure 6) in which overall trends and behaviour of the material can be observed. The plots are spaced so that vertical lines connect points on the scans where signals are exitting the cylinder at the same spot. Reference notation for these plots is shown in Figure 7.

The HT copper cylinder contained a lack of fusion region near the surface 280-310 degrees clockwise from the base of the weld. This affected the scans rcorded at these orientations as well as those on the opposite side of the cylinder, ie in the 100 to 130 degree range. The parts of the scans affected by this crack are shown on the isometric plot (Figure 6h). Figure 8 shows the variations of skew angle with cylinder orientation for all welds. The cyclical (90^{o} period) nature observed particularly in the stainless steel was predicted by Kupperman et al/9/. However, it is less obvious with the other austenitic welds and the copper.

Materials ideally transmit ultrasonic beams in a predictable, consistent manner, as illustrated by the mild steel rod. Results for this material show that the largest amount of the beam energy was transmitted straight through the cylinder with little variation as the cylinder's orientation was changed. The mild steel, titanium grade 2 and 12 welds also exhibited favourable behaviour. On the other hand, considerable beam scatter and skew were found in the results of the stainless steel, copper, Inconel 625 and Hastelloy C-276 welds.

3.3 Analysis of Results

The weld materials were evaluated by taking measurements of plot width, skew angle, and the number of peaks from individual scans (see section 2.3). These values were then combined for each cylinder so that a comparison of behaviour between the welds was possible.

Table 2 shows a summary of the data for all twelve welds. If the mild steel rod is considered an "optimum" material, and the stainless steel a "problem" material, the materials fit fairly well into one or other of these two categories, with only the copper welds as a possible anomoly (due to mechanism rather than results, as shown by the metallography - see section 4.1 below).

Table 3 shows the weld cylinders ranked according to the three criteria (using standard deviation for beam skew ranking). The last two columns show sum of the three rankings and an overall ranking

using all three criteria (a simple arithmetic sum, not based on any theory). Depending on perceived use, either an overall ranking or skew ranking could be used. Fortunately, and not unexpectedly, the materials are fairly consistent through all criteria.

4.0 DISCUSSION

4.1 General Comments

The mild steel and both grades of titanium alloys appear readily inspectable. All show little anisotropy with insignificant beam skewing or spread and only a single peak. In contrast, the stainless steel 316, Inconel 625 and Hastelloy C-276 all show severe anisotropy, with the stainless steel being the least inspectable. This is not unexpected from viewing the microstructures (section 3.1) due to the presence of elongated grains in the z-axis direction. Unfortunately, Kupperman et al/9,10/ have shown the stainless steel behaves rather less anisotropically for longitudinal waves than for shear waves (ie) it is better to inspect stainless steel with longitudinal rather than shear waves. Fortunately, the Inconel and Hastelloy appear less anisotropic than the stainless steel, based on the standard deviation of the beam skew in Table 2.

The copper welds are somewhat different from the stainless, Inconel and Hastelloy welds. Though considerable anisotropy is apparent (Table 2) it appears to come from a different mechanism. Instead of elongated, columnar grains in the z-axis direction, both copper microstructures consist predominately of fairly large, equiaxed grains surrounded by columnar grains from each weld pass (compare figures 4i-4l with 4a, b and 4m-4u). Copper is known to be a fairly "noisy" material to inspect due to its fairly large grains, which agrees with these results.

There was no consistent trend with changing weld interpass temperature in this study. For example, based on the standard deviation of skew angle (ie the variation skewing), there was little difference between the LT and HT titanium grade 12; the copper HT was noticeably better than the copper LT, as was the Hastelloy; however the Inconel LT was better than the Inconel HT. While the predicted trend in grain-size/ultrasonic anisotropy may exist (see section 1.2), this trend may be eclipsed by other factors inherent to the individual welds. For example, copper has such high thermal conductivity that preheat temperature may be almost irrelevant. Put another way, "every weld is different", which has been observed before/12/.

4.2 Future Work Areas

While these results show which materials can be expected to generate inspection problems fairly clearly, the tests were performed using longitudinal waves. Ideally, the same welds should be re-inspected

using shear waves, and preferrably both SV and SH waves since the behaviour of these two types of waves has been shown to be substantially different on stainless steel/9/. Repeating these tests with shear waves will involve using contact probes, and may not be so easy experimentally.

For the titanium diffusion welds, little further characterization is needed at this stage since inspection should generate few material problems. However, there may be considerable practical problems, such as the delivery system (robot, remote manipulator) and coupling method (immersion, waterjet, non-contacting transducer, waterwheel, direct coupling).

For the other welds (copper, stainless steel, Inconel and Hastelloy) further characterization is obviously essential for shear waves. There are a number of techniques such as spatial signal averaging, correct choice of ultrasonic wave, grain-refinement or multiple beam inspection techniques (see section 1.2) which could be developed to improve inspectability. At this stage of the feasibility study, it is probably easiest to summarize by saying that any of the candidate materials except titanium will present some inspection problems. Applied development should wait until a container design has been finalized, and the inspection procedure can be tailored to the final closure weld material and geometry. Further developments for copper, stainless steel, Inconel and Hastelloy are likely to be fairly expensive (probably well over one hundred thousand dollars).

5.0 CONCLUSIONS

1. Ultrasonic inspections of cylinders of weld metal from candidate used fuel container materials using longitudinal waves showed the following:

   (a) titanium grade 2 and 12 showed essentially isotropic behaviour,

   (b) commercially-pure copper, 316 stainless steel, Inconel 625 and Hastelloy C-276 showed significant anisotropy (ie) beam skewing and spread;

   (c) altering interpass temperatures had no consistent effect.

2. Numerical/statistical procedures were used to rank these materials. Using the most important criterion (beam skew) the order was titanium grade 2 (best)>mild steel>titanium Gr 12 HT>titanium Gr 12 LT>>Inconel LT>Copper HT>Hastelloy HT>Inconel LT>Hastelloy LT>Copper LT>stainless steel (worst) [HT and LT designate high temperature and low temperature interpass welds].

3. Metallography showed that the stainless steel, Inconel and Hastelloy welds all had large columnar grains in the out-of-weld plane. In contrast, the copper showed columnar grains round each weld pass and equiaxed grains in the weld pass centres.

4. Titanium (either grade 2 or 12) fusion welds should present few material inspection problems, but copper, stainless, Inconel or Hastelloy will. Further development work can be anticipated for the latter materials.

6.0 RECOMMENDATIONS

1. Perform beam skewing measurements on the candidate weld materials using shear wave ultrasonics (SV and SH).

2. Perform initial studies on coupling ultrasound using waterjets or waterwheels, rather than using full immersion.

ACKNOWLEDGEMENTS

The welds were manufactured by Union Carbide-Linde, the Welding Institute of Canada and the Titanium Company. Metallography was performed by Mr. F. Smith in Metallurgical Services. Mr. A.L. Allen assisted with the ultrasonics. This project is part of the Technical Assistance Program with Atomic Energy of Canada Ltd on the Canadian Nuclear Fuel Waste Management Program.

Recommended:

J.A. Baron
Supervising Engineer
Nondestructive & Fracture
Evaluation Section

Approved:

O.A. Kupcis
Manager
Metallurgical Research Dept

Prepared:

M.D.C. Moles
Engineer-NDE
Nondestructive & Fracture
Evaluation Section

FOR. J. Imada
Co-op Student
University of Waterloo

Reviewed:

J.A. Chadha
Area Co-ordinator
AECL Technical Assistance Program

REFERENCES

1. K. Nuttall, J.L. Crosthwaite, P.J. McKay, P.M. Mathew, B. Teper, P.Y.Y. Maak and M.D.C. Moles, Materials Research Society 6th International Symposium on the Scientific Basis for Nuclear Waste Management, Boston, MA. November 1-4, 1982.

2. K. Nuttall, Proceedings of the Fourteenth Information Meeting of the Nuclear Fuel Waste Mangement Program (1982 General Meeting), Winnipeg, Manitoba, September 15-16, 1982. (Also AECL Technical Record TR-207, December 1982).

3. G.J. Dau, I. Mech. E. Conference Paper C212/76, 1976.

4. B.R. Dewey, L. Adler, R.T. King and K.V. Cook, Experimental Mechanics, November 1977, p. 420.

5. S.J. Mech, J.S. Emmons, and T.E. Michaels, Proceedings of the First International Symposium on Ultrasonic Materials Characterization, Gaithersburg, Maryland, June 7-9, 1978. Issued as NBS Special Publication 596, September 2980, p. 561.

6. L. Adler, K.V. Cook and D.W. Fitting, idem, p. 533.

7. M.G. Silk, Materials Evaluation, vol 39, April 1981, p. 462.

8. D.S. Kupperman, K.J. Reimann and N.F. Fiore, Materials Evaluation, April 1978, p. 70.

9. D.S. Kupperman and K.J. Reimann, IEEE Transactions on Sonics and Ultrasonics, vol SU-27, No. 1, January 1980, p. 7.

10. D.S. Kupperman, K.J. Reimann and D.I. Kim, Proceedings of Symposium on "Nondestructive Evaluation: Microstructural Characterization and Reliability Strategies", sponsored by TMS-AIME and ASM, Pittsburgh, PENN, October 5-9, 1980, Ed. by O. Buck and S.M. Wolf, p. 199.

11. D.S. Kupperman, K.J. Reimann and A. Winiecki, Materials Evaluation, Vol 39, May 1981, p. 527.

12. P. Caussin, J. Cermak and D. Verspeelt, 4th International Conference on Nondestructive Evaluation in the Nuclear Industry, Lindau, West Germany, May 25-27, 1981.

13. X. Edelmann, NDT International, June 1981, p. 1.

14. M.G. Silk, Ultrasonics, September 1981, p. 208.

15. M.K. Murali and K. Neelakantan, NDT International, December 1981, p. 321.

16. D. Heinrich, G. Muller nd M. Weiss, NDT International, August 1982, p. 179.

17. D.S. Kupperman, K.J. Reimann and D. Yuhas, Proceedings of Conf. on "Quantitative NDE in the Nuclear Industry", Publ. by American Society for Metals, Metals Park, OH (1983), San Diego, Calif, May 1982, p. 172.

18. L.A. Lott and R.K. Malik, Materials Evaluation, vol 41, May 1983, p. 738.

19. J. Tomlinson, A. Wagg and M. Whittle, Proceedings of International Conference on "Nondestructive Evaluation in the Nuclear Industry, Salt Lake City, Utah, February 13-15, 1978, p. 64.

20. A. Singh, Ultrasonics, November 1983, p. 270.

TABLE 1: WELDS PREPARED

MATERIAL	INTERPASS TEMPERATURE	NUMBER OF PASSES
Mild Steel	99-260°C	17
316L Stainless Steel	29-149°C	21
Titanium Grade 2	66-93°C	56
Titanium Grade 12	21°C	56
Titanium Grade 12	66-93°C	56
Copper C11000	149°C	17
Copper C11000	260°C	16
Inconel 625	135-154°C	53
Inconel 625	260-371°C	54
Hastelloy C-276	21°C	53
Hastelloy C-276	148°C	49

TABLE 2: SUMMARY OF MEASUREMENTS FOR EACH CYLINDER

CYLINDER	PLOT WIDTH (°) Average	PLOT WIDTH (°) Standard Deviation	SKEW ANGLE (°) Average	SKEW ANGLE (°) Standard Deviation	WEIGHTED AVERAGE NUMBER OF PEAKS
Mild Steel Rod	50.81	0.82	1.23	1.23	1.0
Mild Steel Weld	55.14	5.22	2.33	2.24	1.0
Stainless Steel	74.93	36.53	8.15	27.53	2.5
Titanium Gr. 2	50.57	1.13	1.39	1.40	1.0
Titanium Gr. 12 LT	49.64	3.55	2.11	3.47	1.0
Titanium Gr. 12 HT	47.80	2.26	2.19	3.42	1.0
Copper LT	69.66	17.77	3.70	18.05	2.6
Copper HT	56.94	15.69	4.85	11.40	1.9
Inconel 625 LT	71.51	25.20	0.68	10.97	2.1
Inconel 625 HT	76.94	24.14	0.00	15.23	2.6
Hastelloy C-276 LT	76.56	27.28	3.57	17.71	2.5
Hastelloy C-276 HT	72.17	24.64	3.49	14.02	2.0

TABLE 3: CYLINDER RANKING

Cylinder	Width Ranking	Skew Ranking	# of Peaks Rankings	Sum of 3 Rankings	Overall Ranking
Mild Steel	1	1	1	3	1
Mild Steel Weld	5	3	1	9	4
Stainless Steel	12	12	9	33	12
Titanium Gr. 2	2	2	1	5	2
Titanium Gr. 12 LT	4	5	1	10	5
Titanium Gr. 12 HT	3	4	1	8	3
Copper LT	7	11	11	29	9
Copper HT	6	7	6	19	6
Inconel LT	9	6	8	23	7
Inconel HT	10	9	11	30	10
Hastelloy LT	11	10	9	30	10
Hastelloy HT	8	8	7	23	7

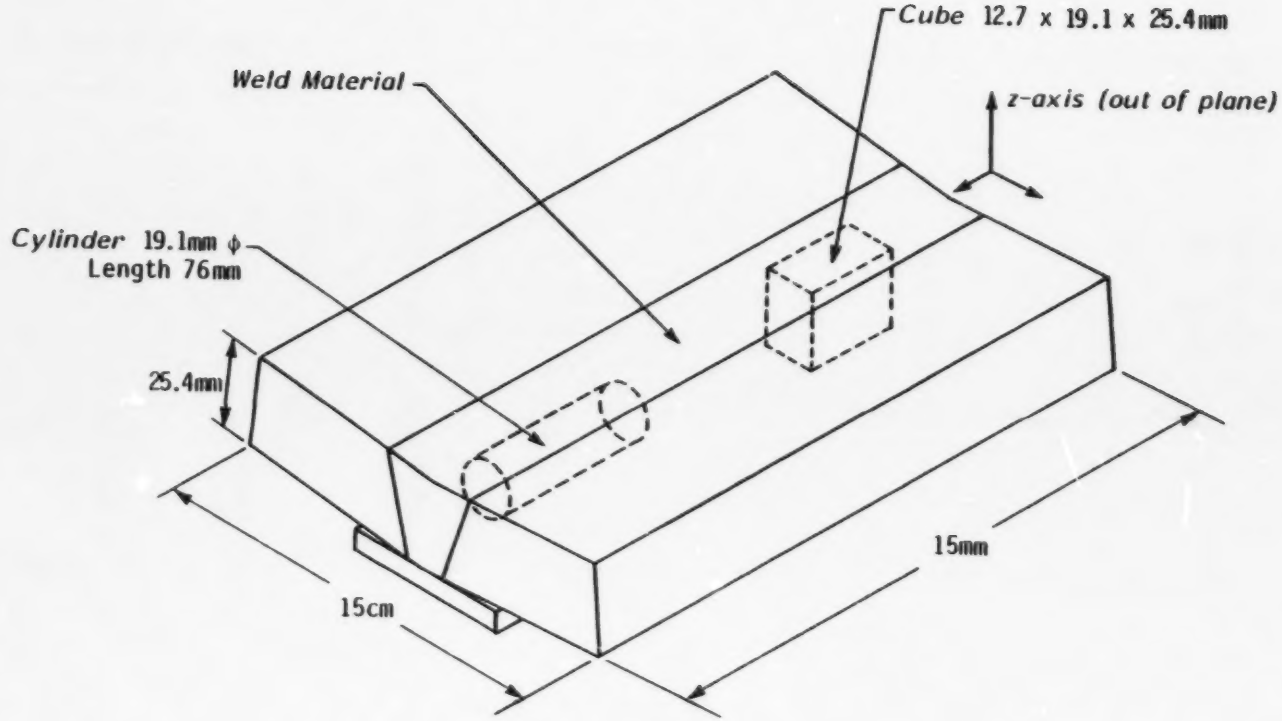

FIGURE 1
WELD LAYOUT

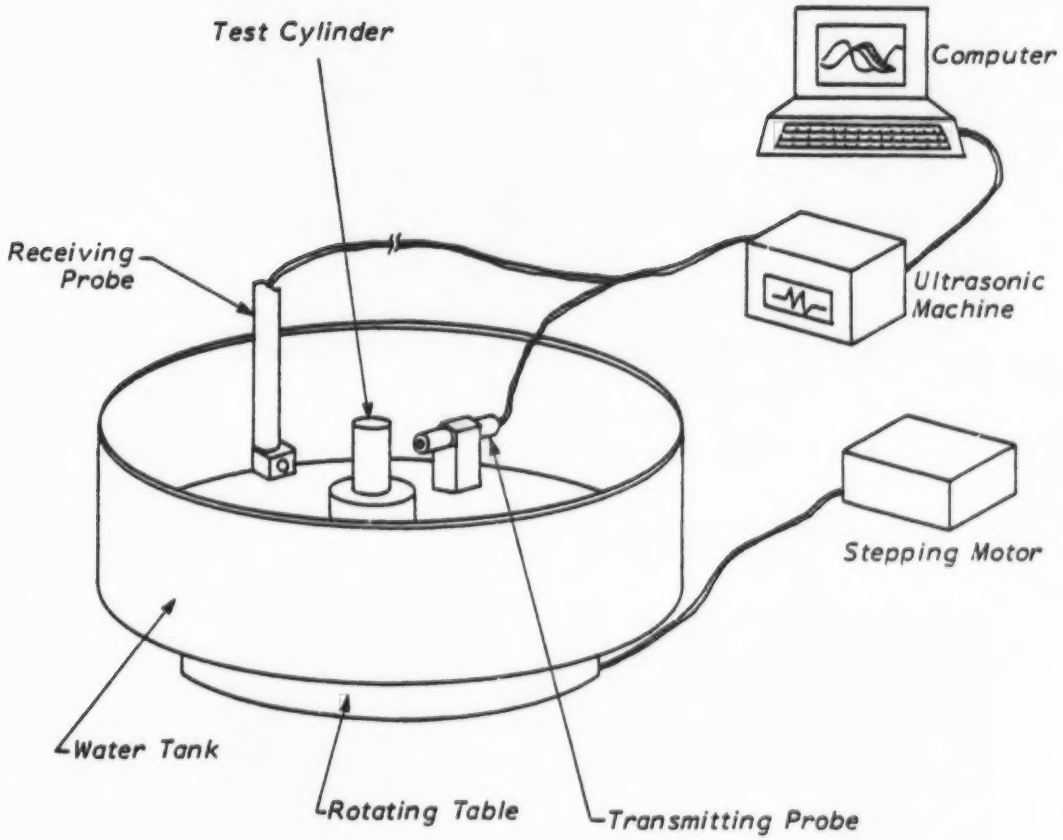

- *Equipment List:*

1)	*Transmitting Probe:*	*Aerotech Alpha*	25MHz, 0.25"ϕ, 2.0" Focus
2)	*Receiving Probe:*	*Aerotech Alpha*	10MHz, 0.25"ϕ, 2.0" Focus
3)	*Ultrasonic Machine:*	*Krautkrämer*	USIP11
4)	*Computer:*	*Apple II Plus*	

- *Distance of Receiving Probe from Face of Cylinder:* 34.3 mm
- *Distance of Transmitting Probe from Face of Cylinder:* 38.8 mm

FIGURE 2
EQUIPMENT SETUP

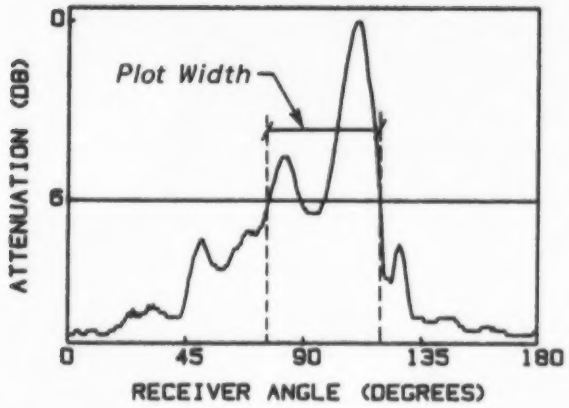

(a)
Plot Width

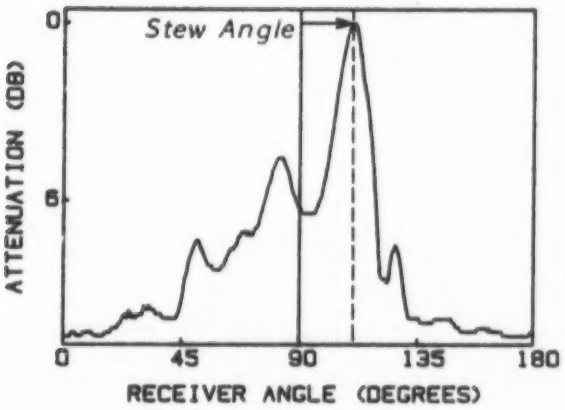

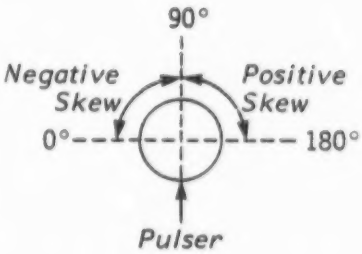

(b)
Skew Angle

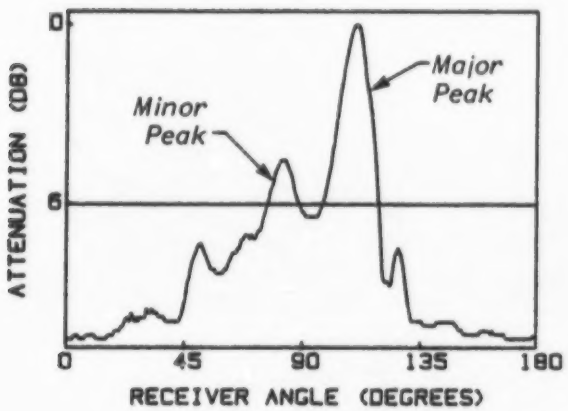

(c)
Number of Peaks

FIGURE 3
THE THREE INDIVIDUAL SCAN MEASUREMENTS

165206 RD

Z-AXIS

1 mm

FIGURE 4(a)

STAINLESS STEEL (x 5)

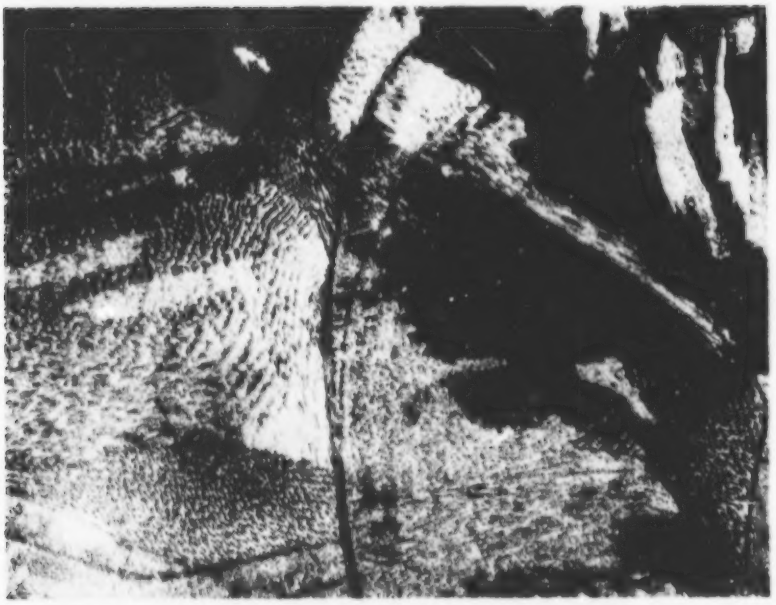

0.1 mm

FIGURE 4(b)

STAINLESS STEEL WELD (x 20)

165754 RD

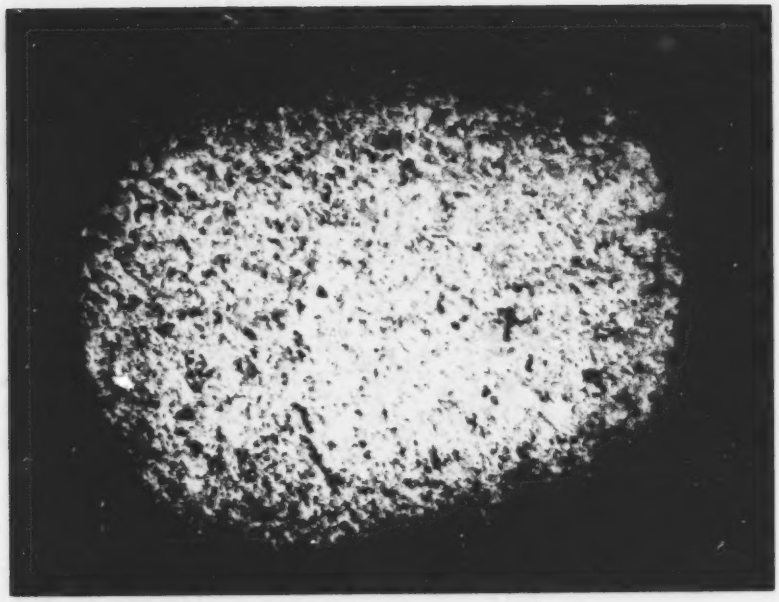

1 mm

FIGURE 4(c)

TITANIUM GRADE 2 WELD (x 5)

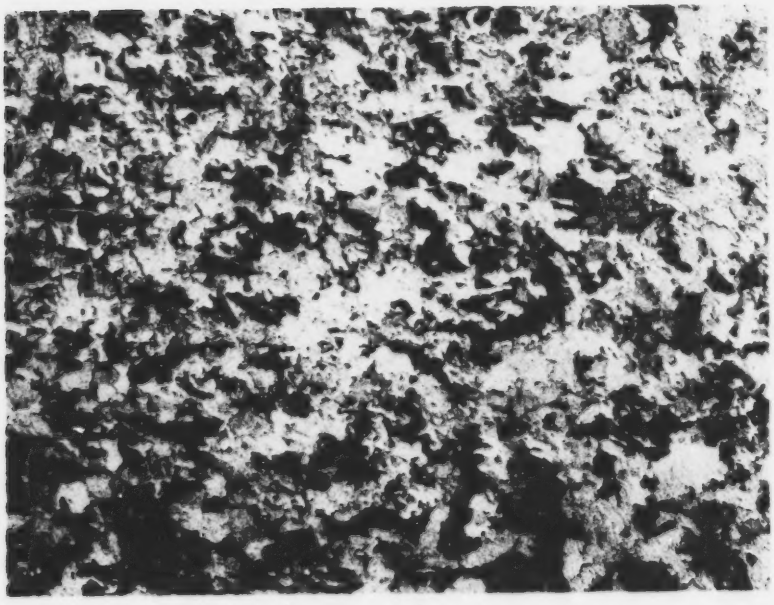

0.1 mm

FIGURE 4(d)

TITANIUM GRADE 2 WELD (x 20)

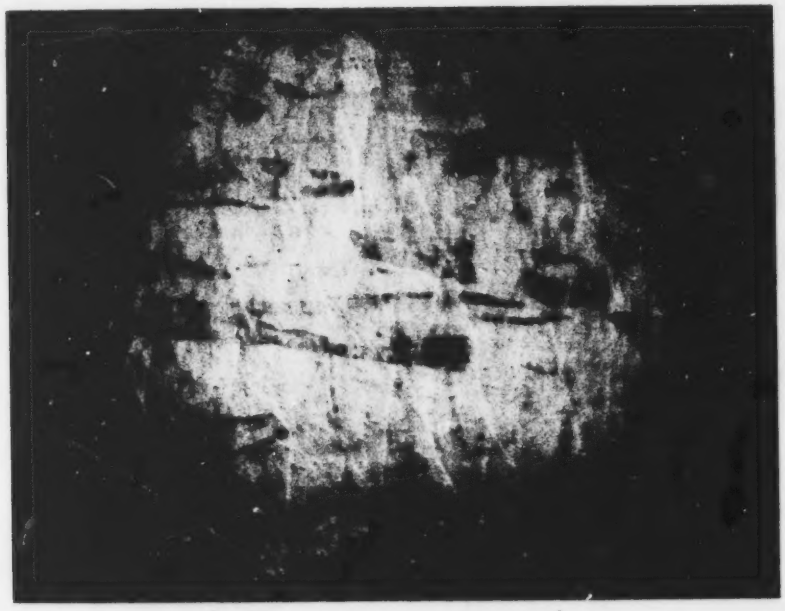

FIGURE 4(e)
TITANIUM GRADE 12 WELD, LT (x 5)

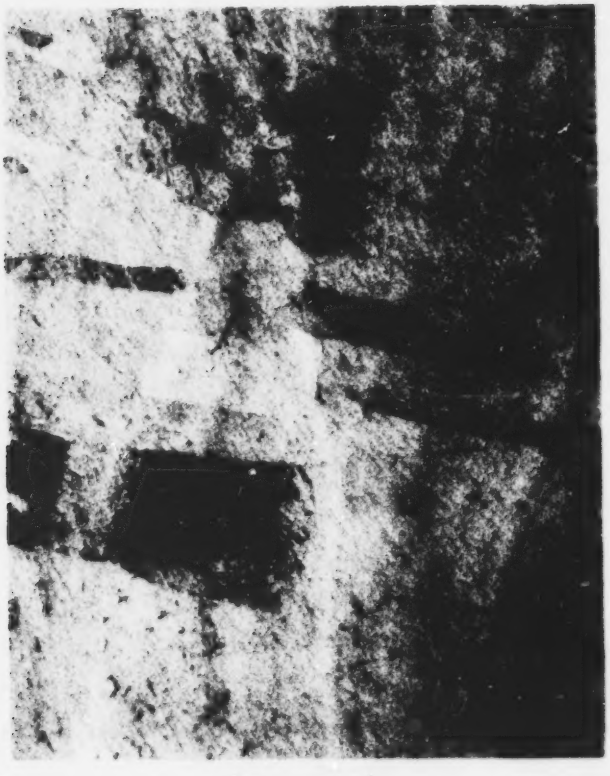

FIGURE 4(f)
TITANIUM GRADE 12 WELD, LT (x 20)

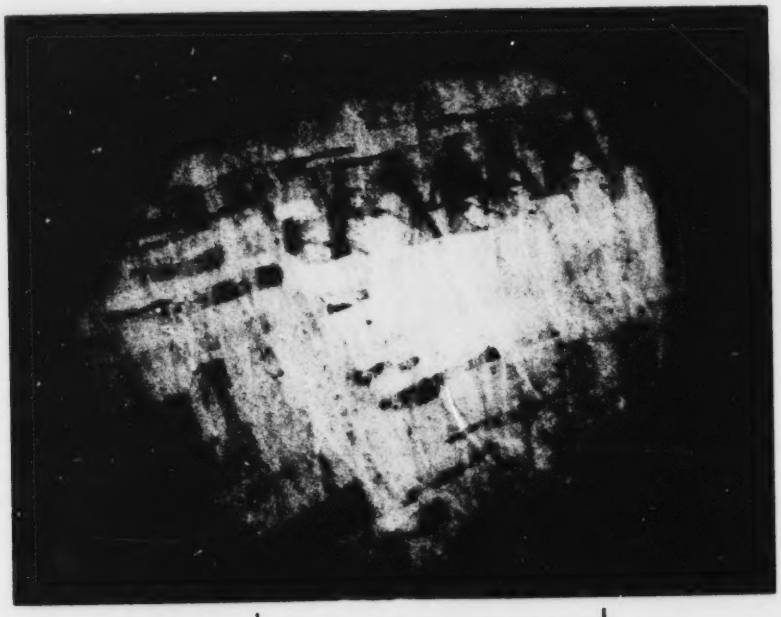

FIGURE 4(g)
Ti GRADE 12 HT WELD (x 5)

FIGURE 4(h)
Ti GRADE 12 HT WELD (x 20)

FIGURE 4(i)

LT COPPER WELD (x 5)

FIGURE 4(j)

LT COPPER WELD (x 20)

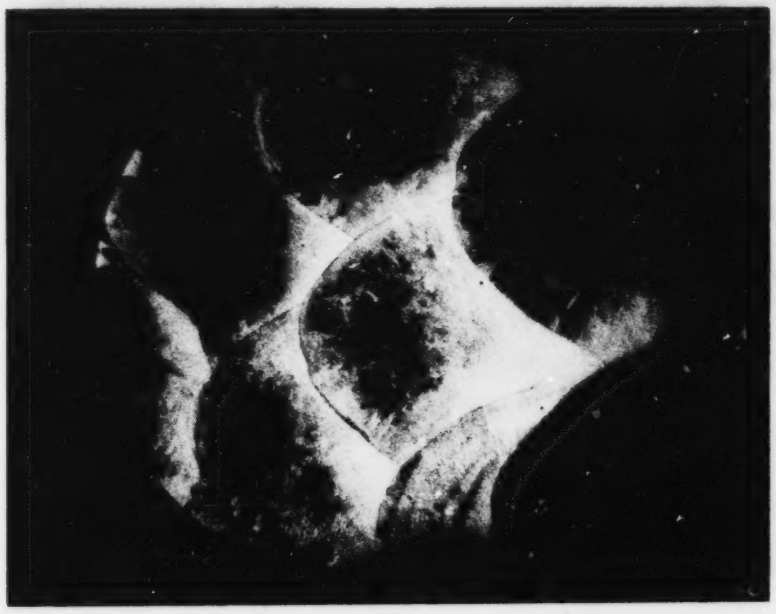

1 mm

FIGURE 4(k)

HT COPPER WELD (x 5)

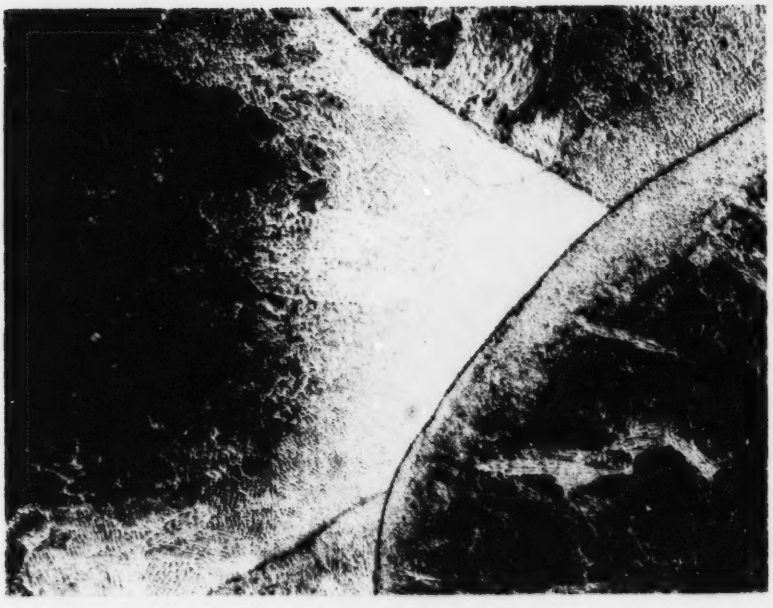

0.1 mm

FIGURE 4(l)

HT COPPER WELD (x 20)

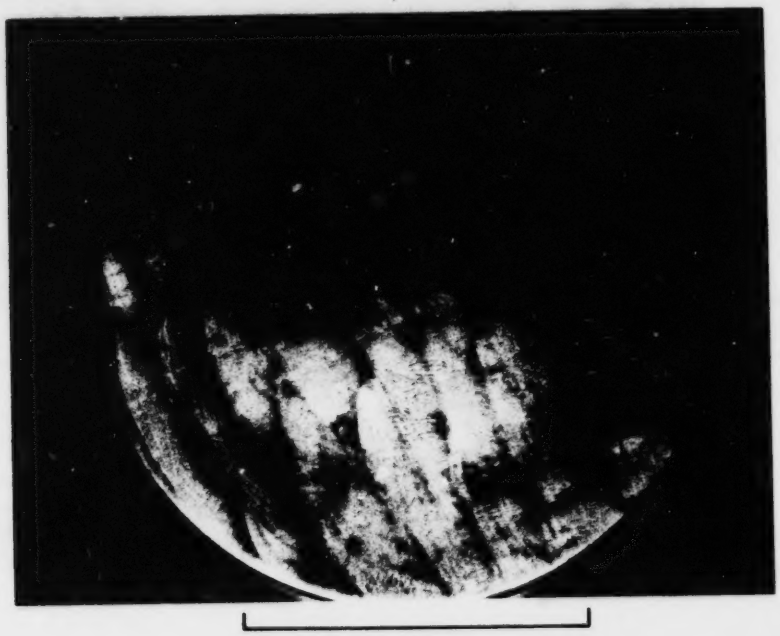

FIGURE 4(m)
LT INCONEL 625 WELD (x 5)

FIGURE 4(n)
LT INCONEL 625 WELD (x 20)

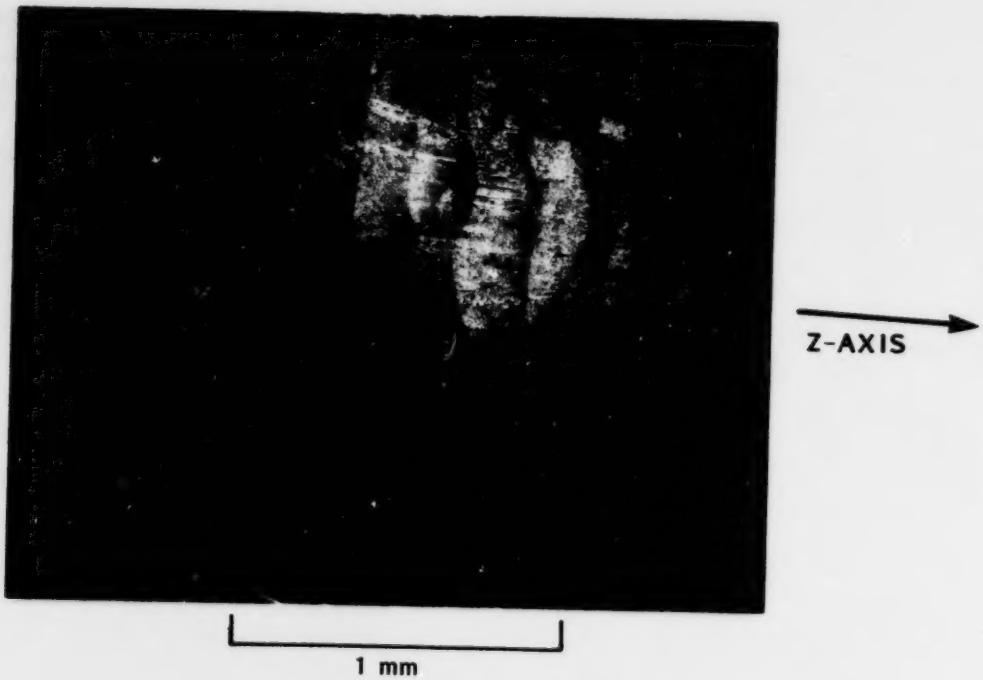

FIGURE 4(o)
HT INCONEL 625 WELD (x 5)

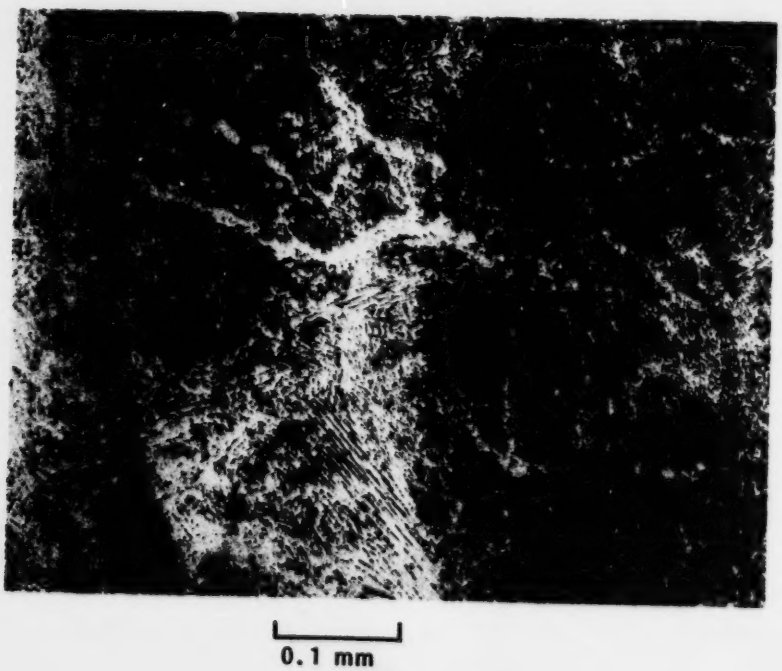

FIGURE 4(p)
HT INCONEL 625 WELD (x 20)

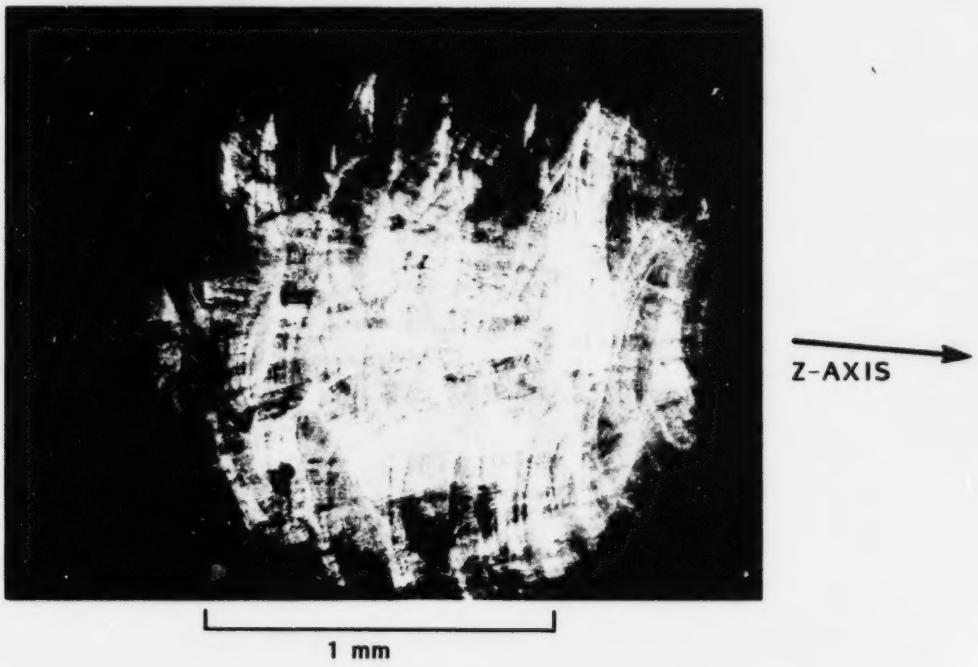

FIGURE 4(r)
LT HASTELLOY C-276 WELD (x 5)

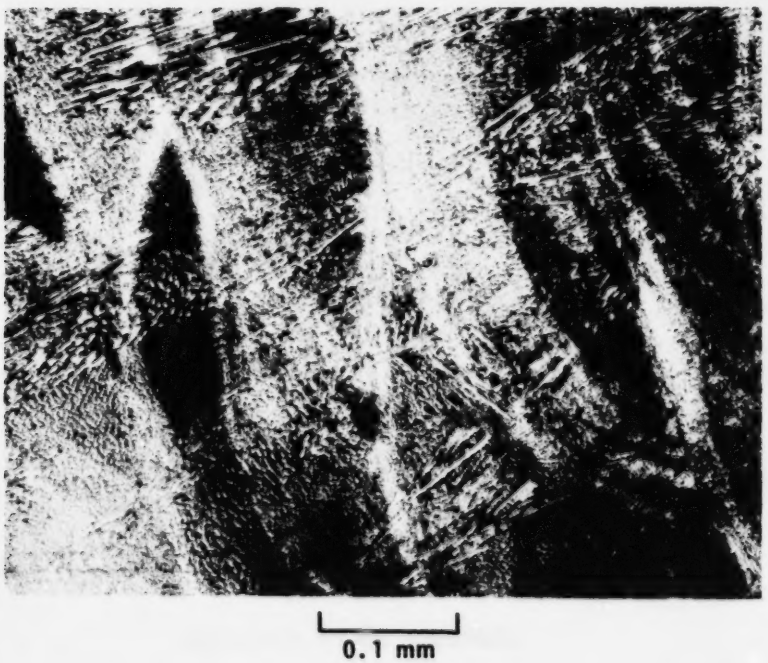

FIGURE 4(s)
HASTELLOY C-276 WELD (x 20)

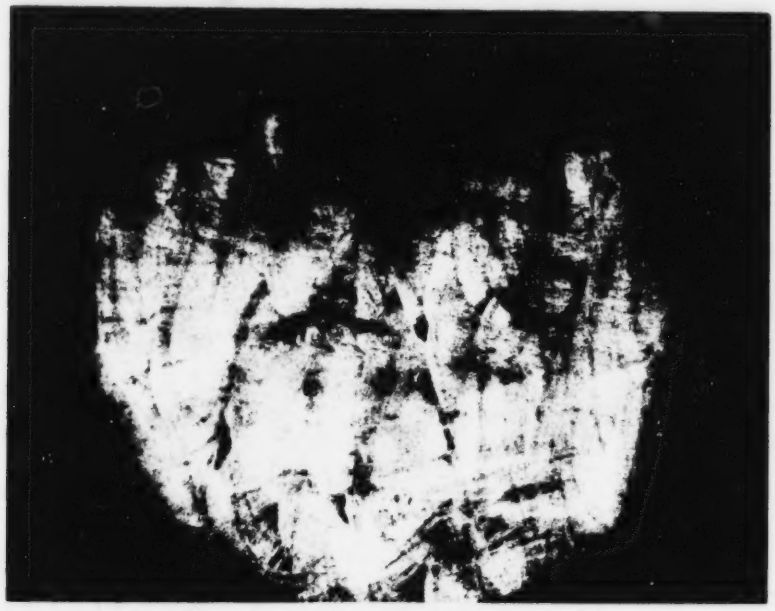

FIGURE 4(t)
HT HASTELLOY C-276 WELD (x 5)

FIGURE 4(u)
HT HASTELLOY C-276 WELD (x 20)

FIGURE 5 : Sample Plots Generated from Scans

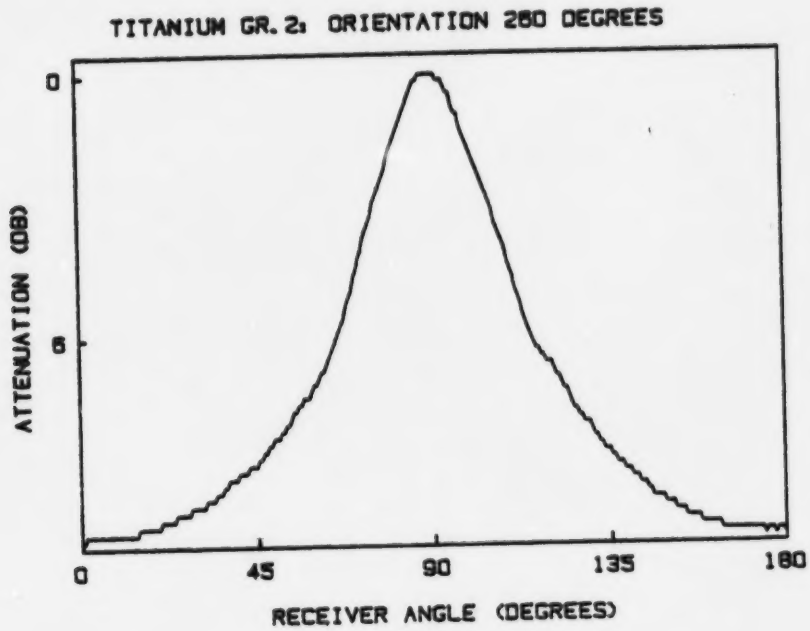

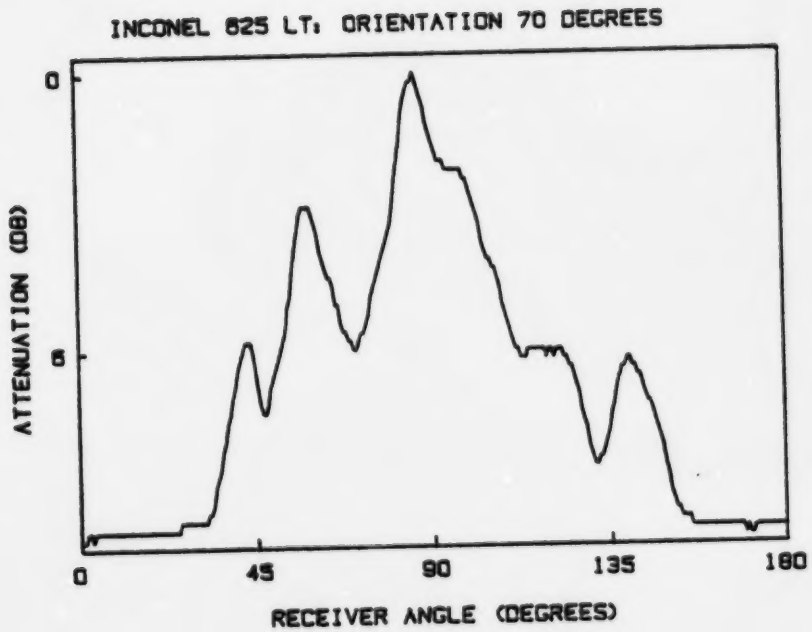

165764 RD

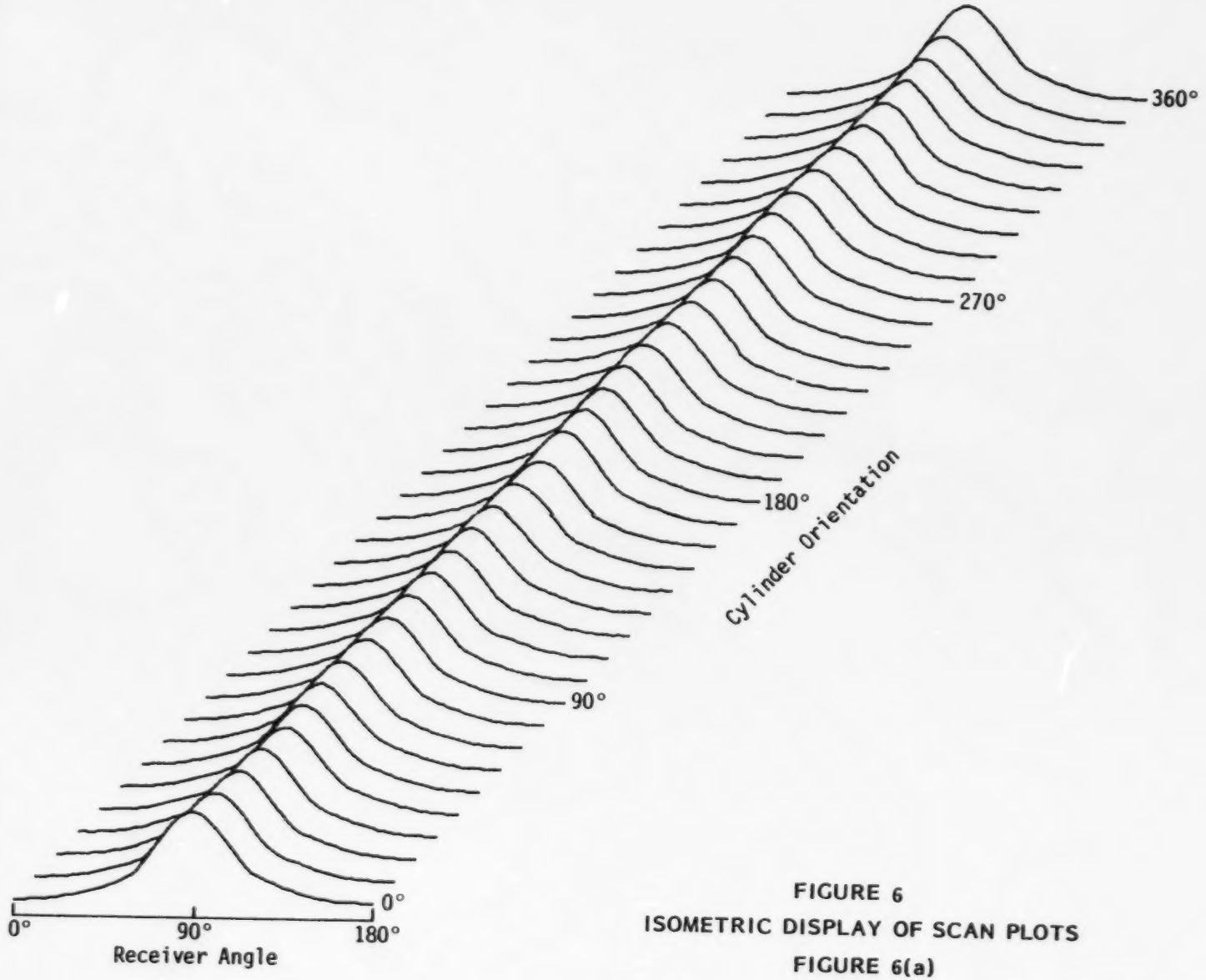

FIGURE 6
ISOMETRIC DISPLAY OF SCAN PLOTS
FIGURE 6(a)
MILD STEEL

165193 RD

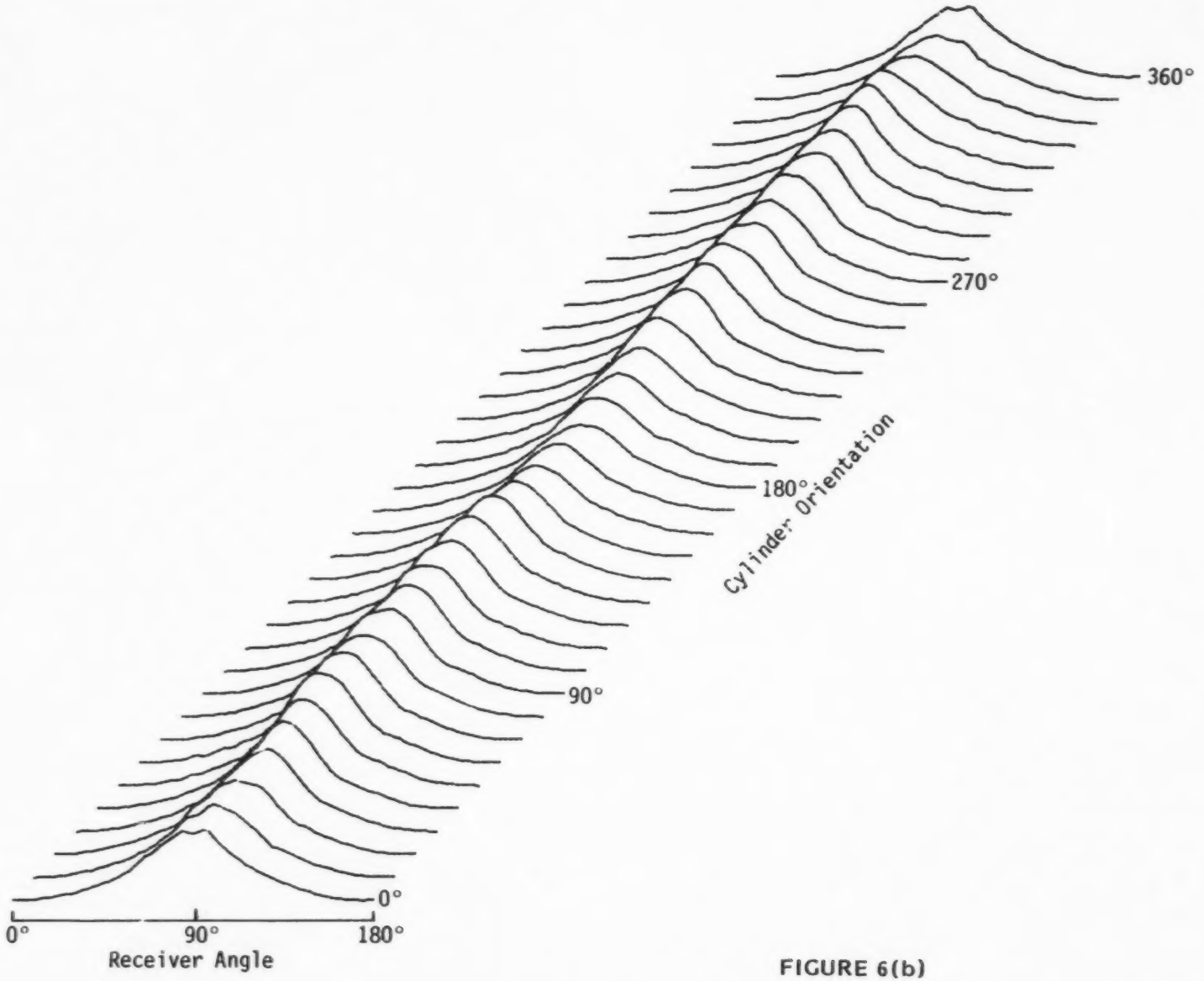

FIGURE 6(b)
MILD STEEL WELD

165194 RD

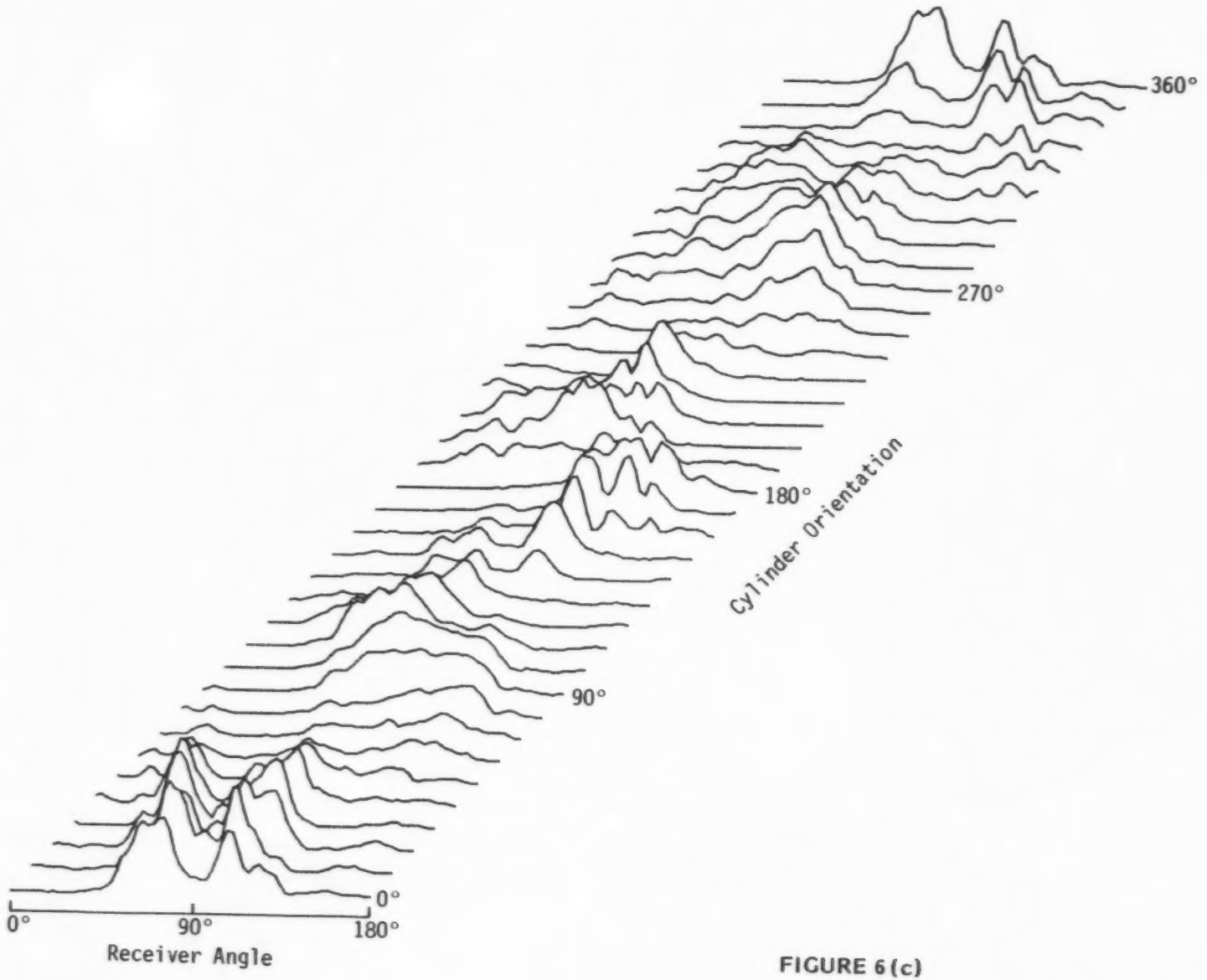

165195 RD

FIGURE 6(c)
STAINLESS STEEL

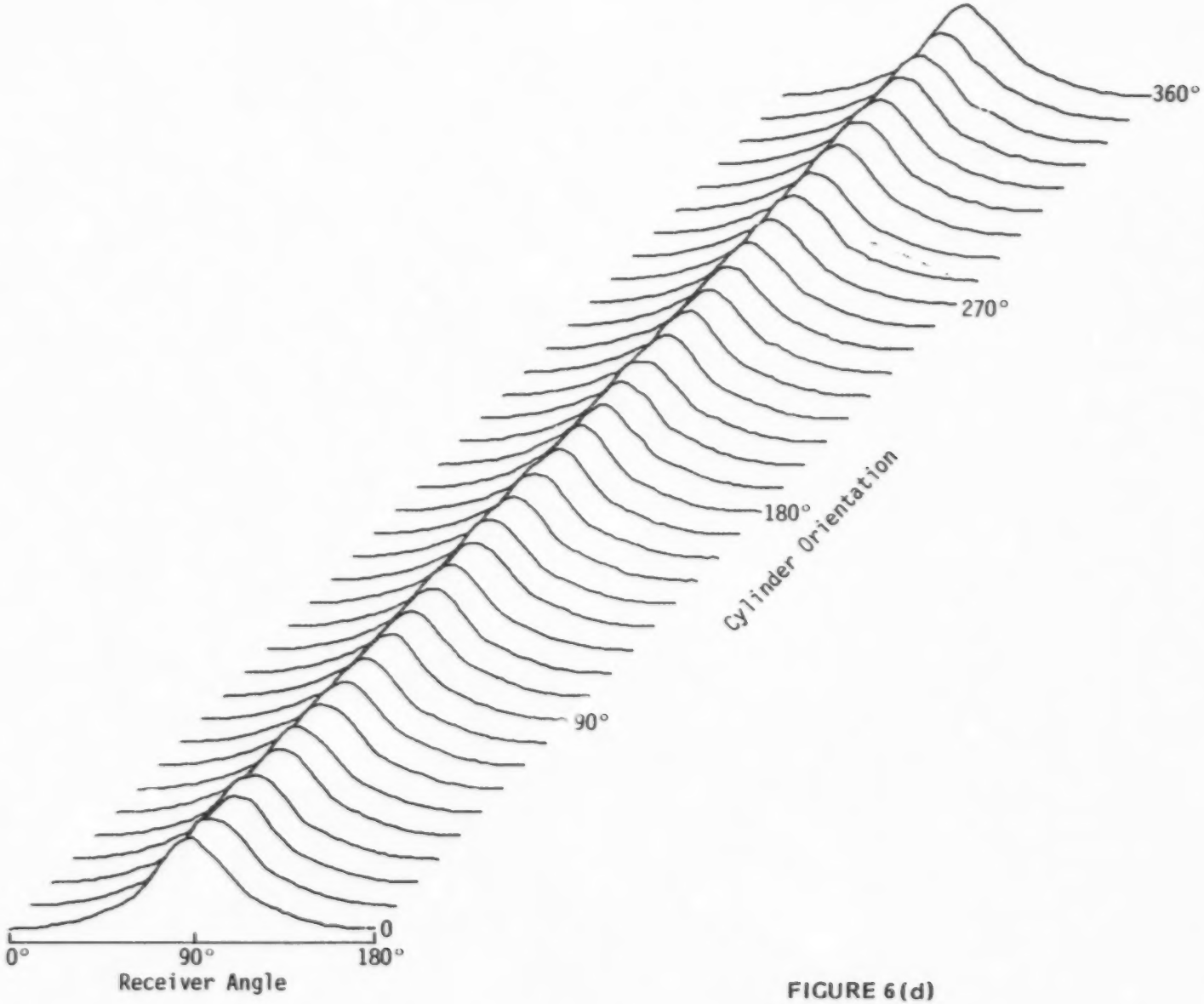

165196 RD

FIGURE 6(d)
TITANIUM GR.2

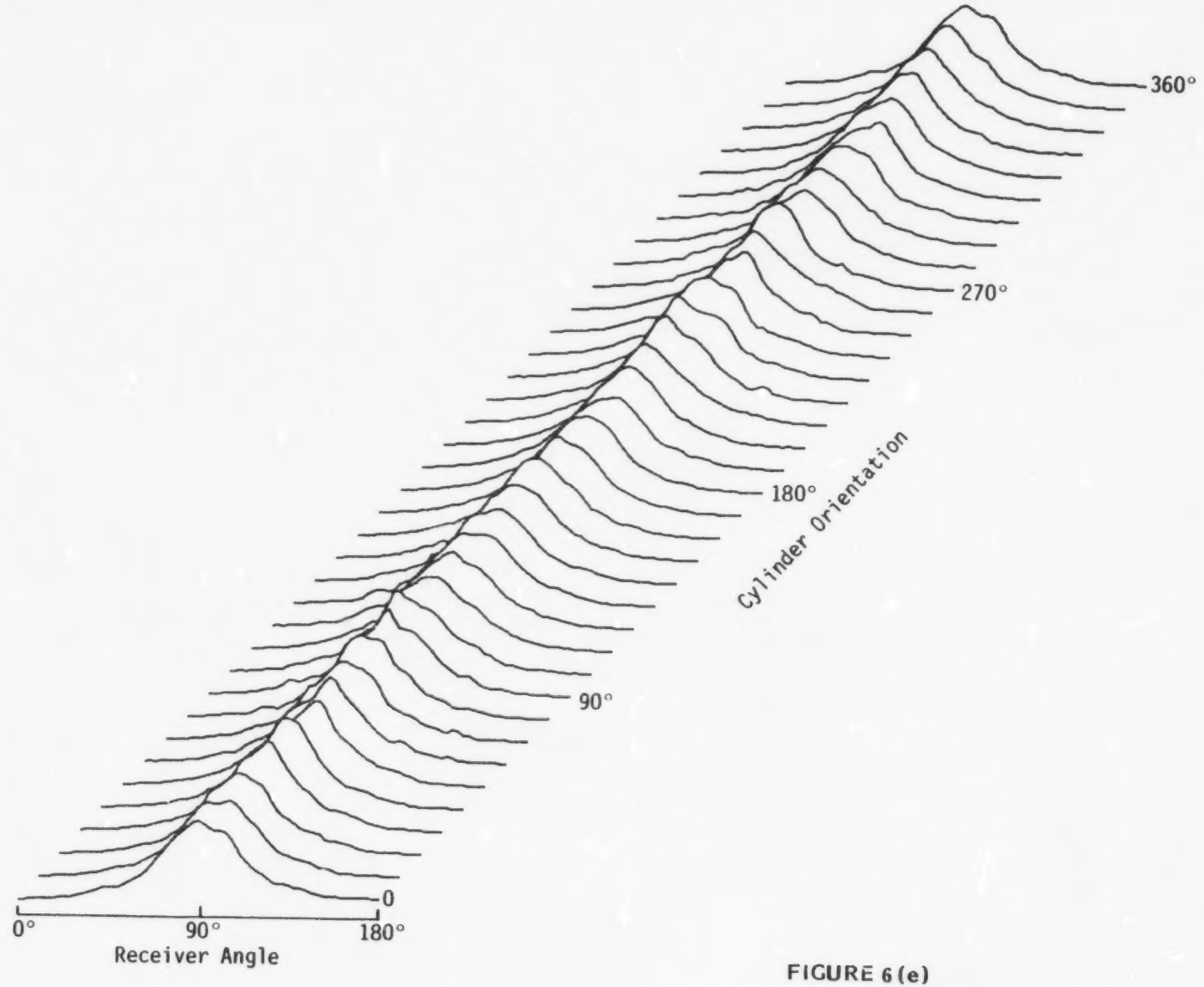

165197 RD

FIGURE 6(e)
TITANIUM GR.12 LT

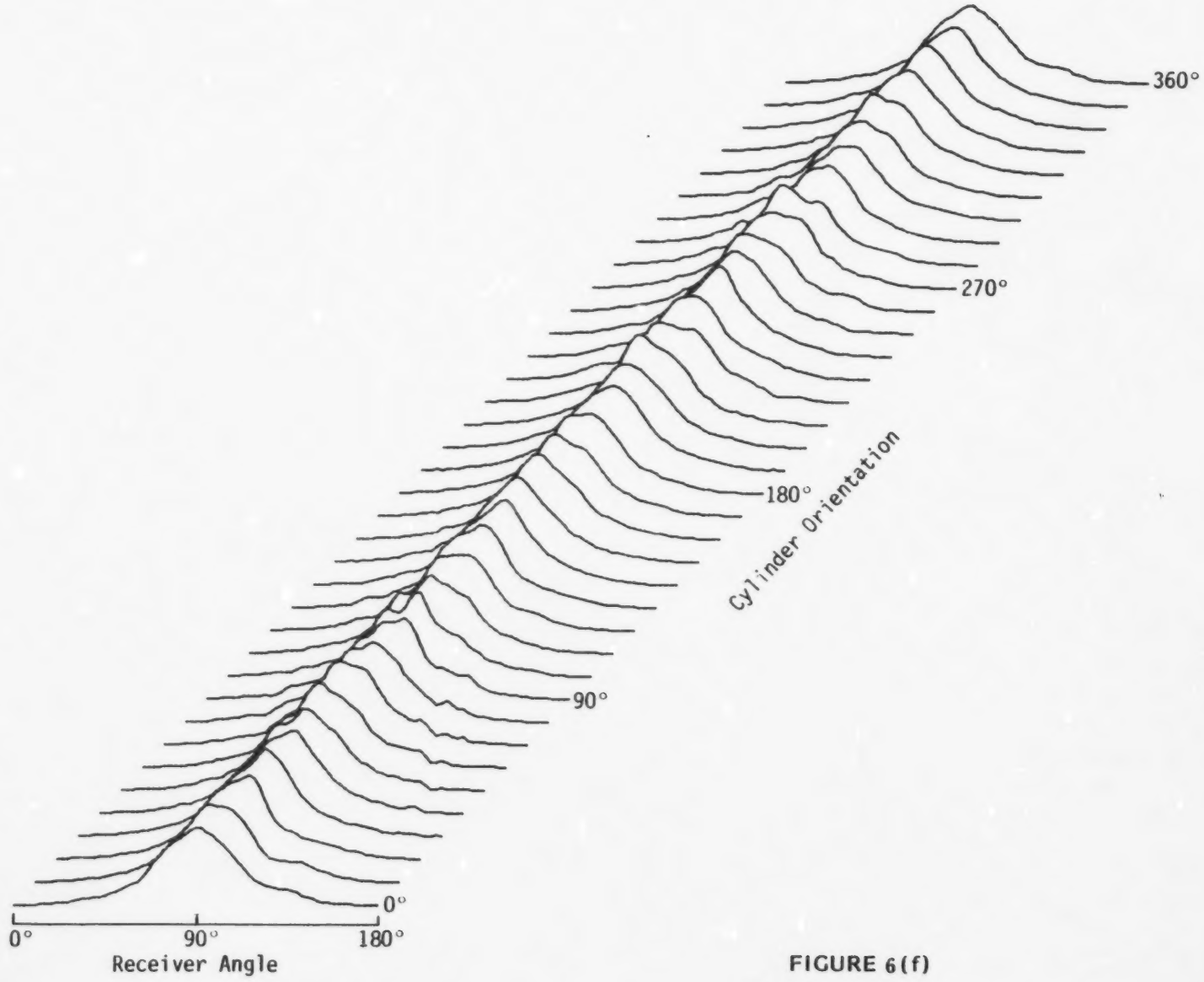

FIGURE 6(f)
TITANIUM GR. 12 HT

165198 RD

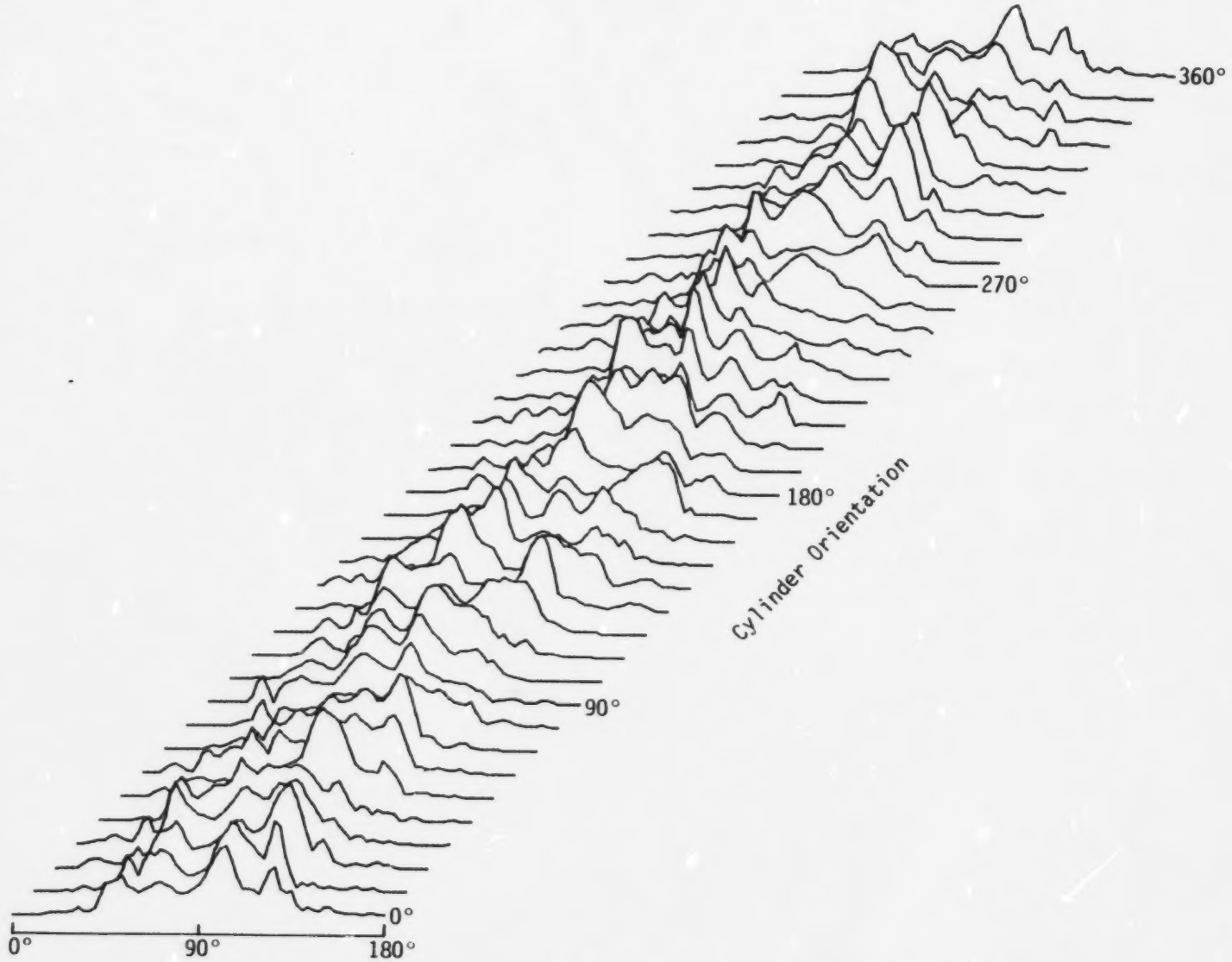

165199 RD

FIGURE 6(g)
COPPER LT

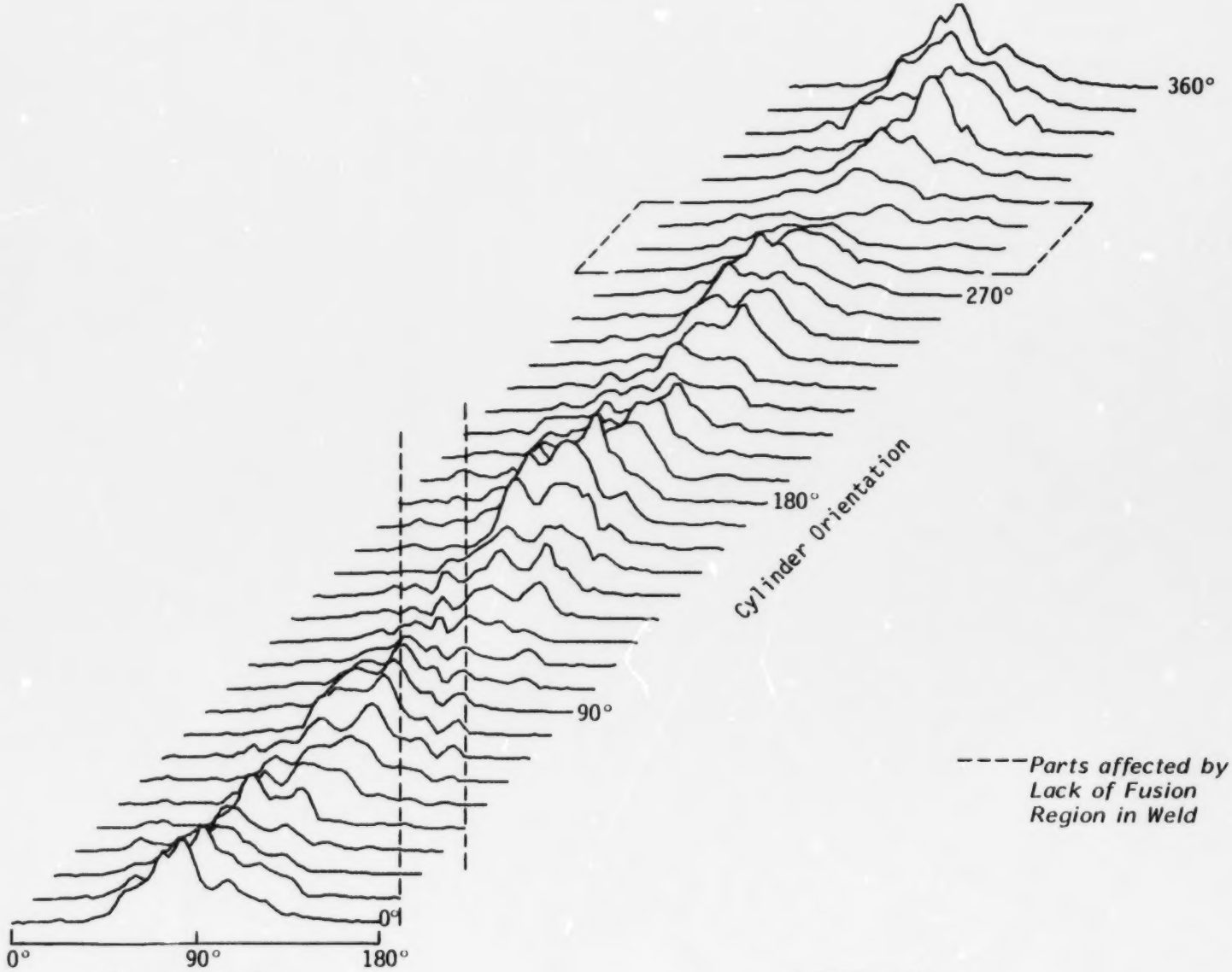

165200 RD

FIGURE 6(h)
COPPER HT

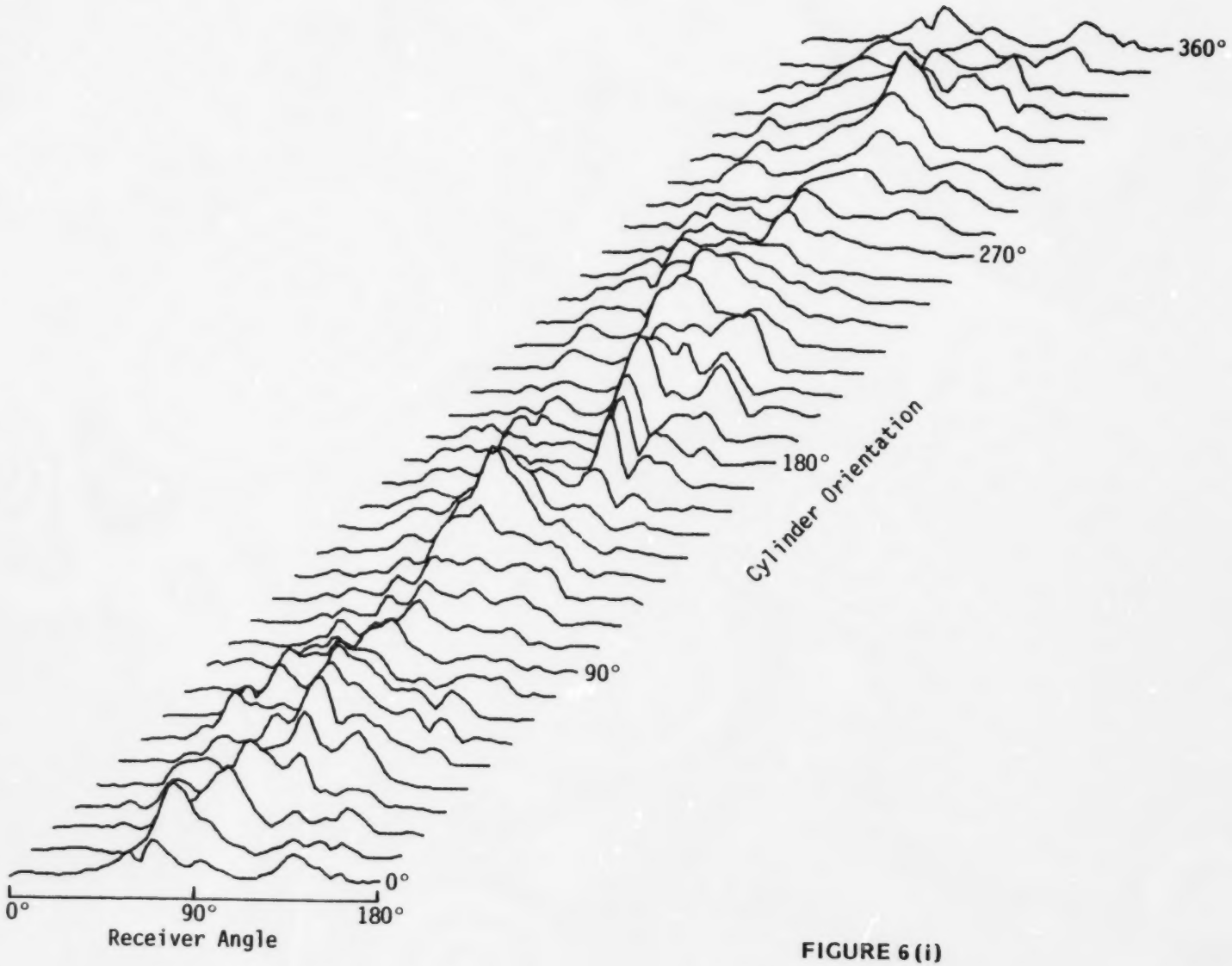

165201 RD

FIGURE 6 (i)
INCONEL 625 LT

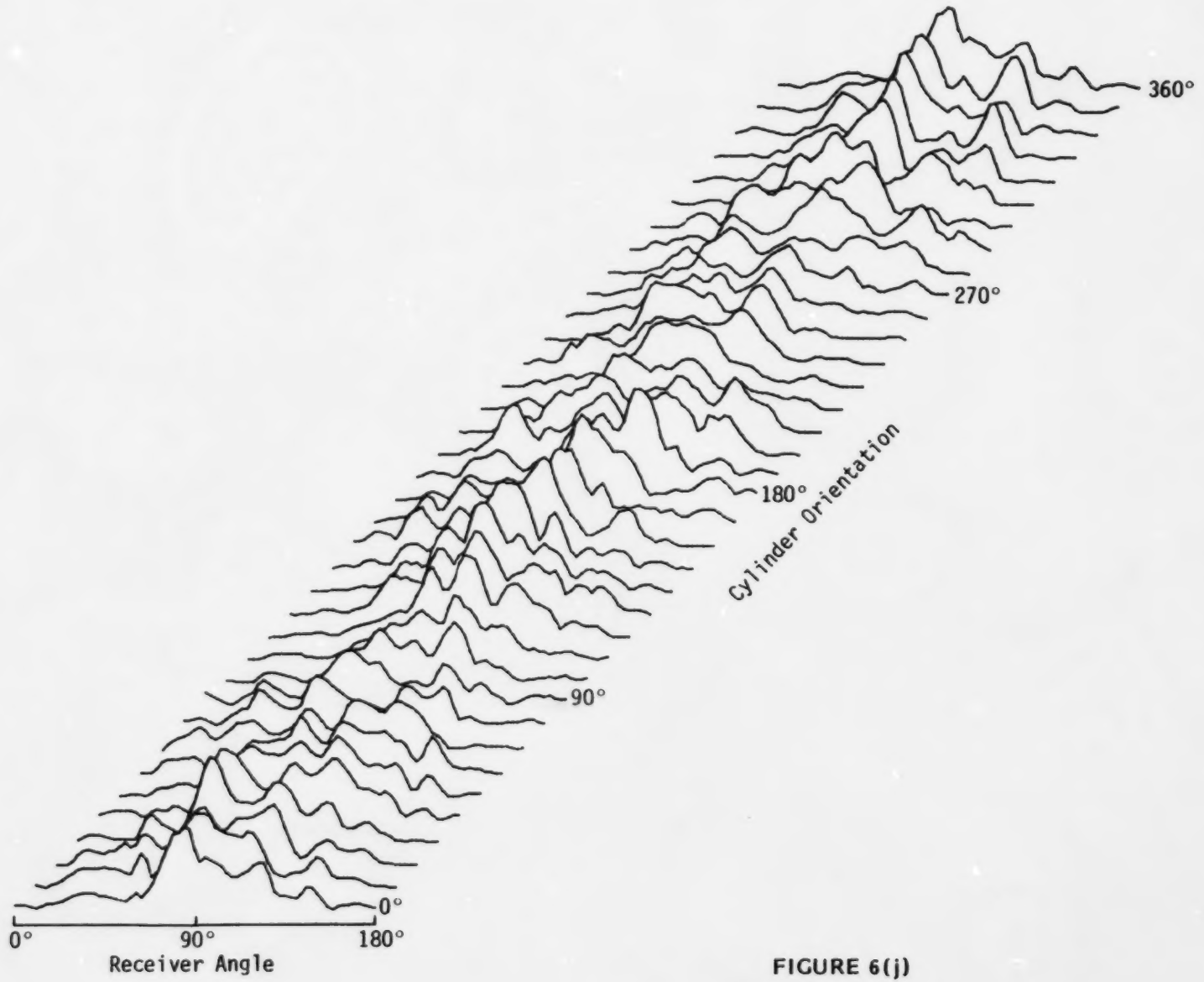

165202 RD

FIGURE 6(j)
INCONEL 625 HT

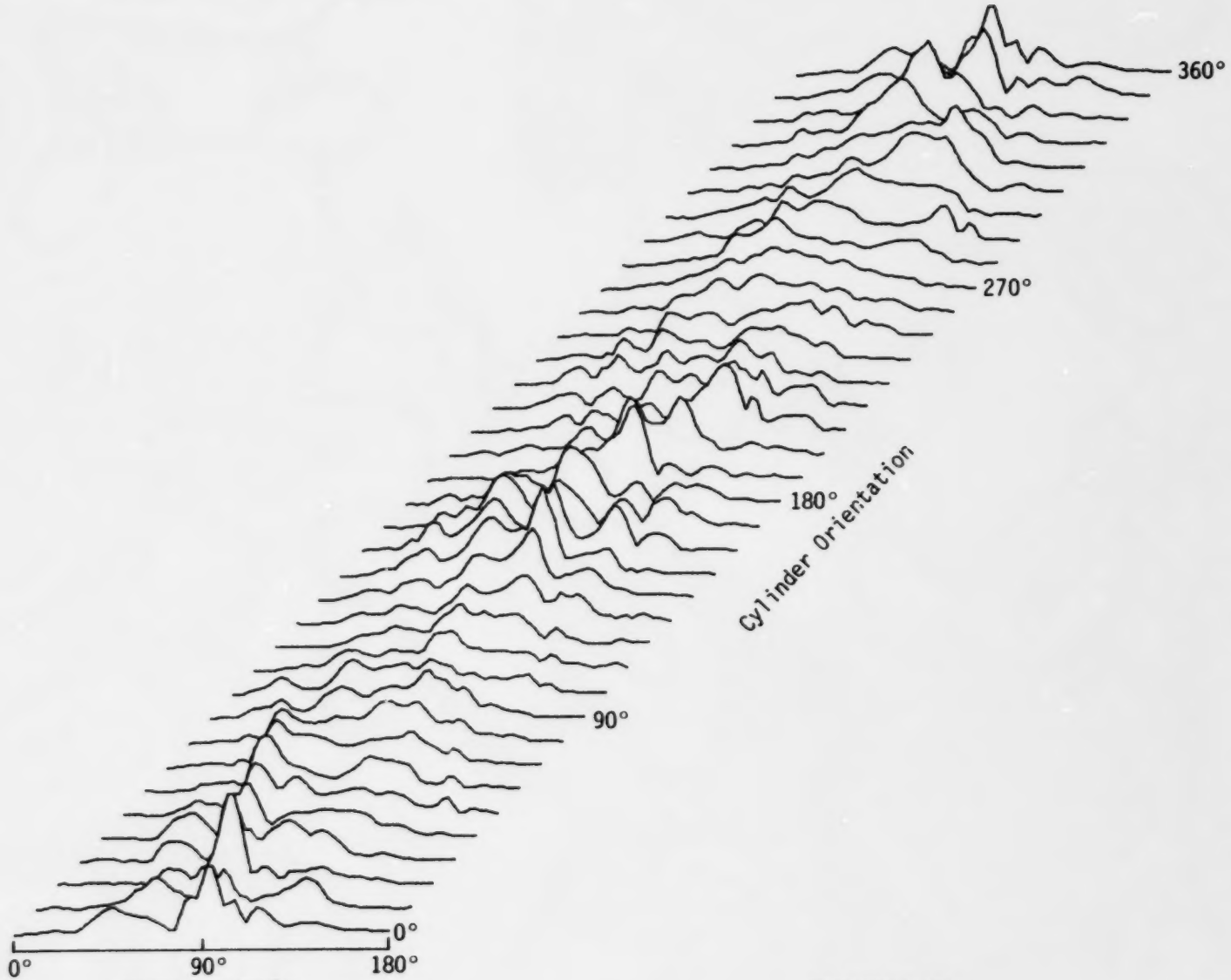

165203 RD

FIGURE 6 (k)
HASTELLOY C-276 LT

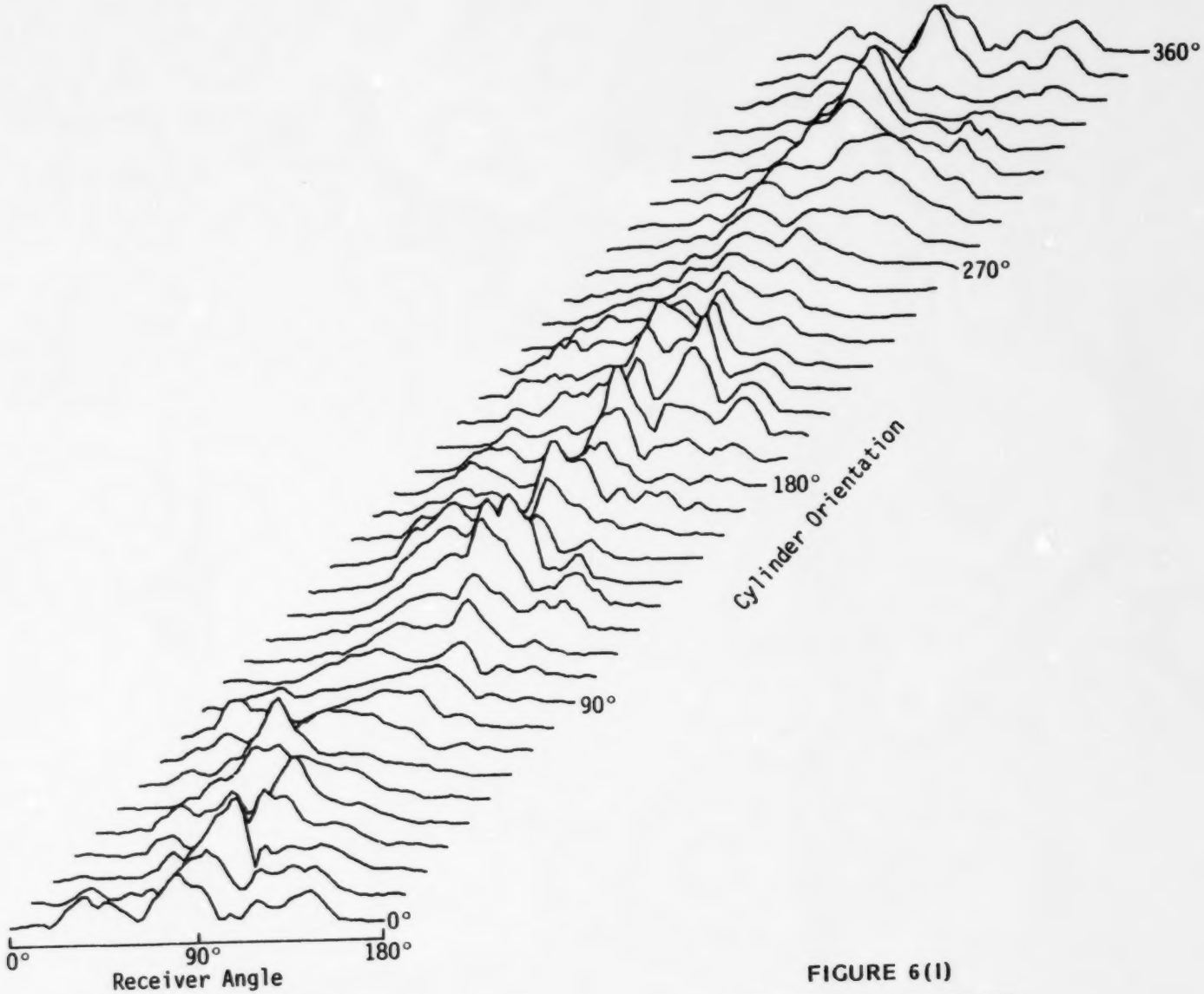

FIGURE 6(I)
HASTELLOY C-276 HT

165204 RD

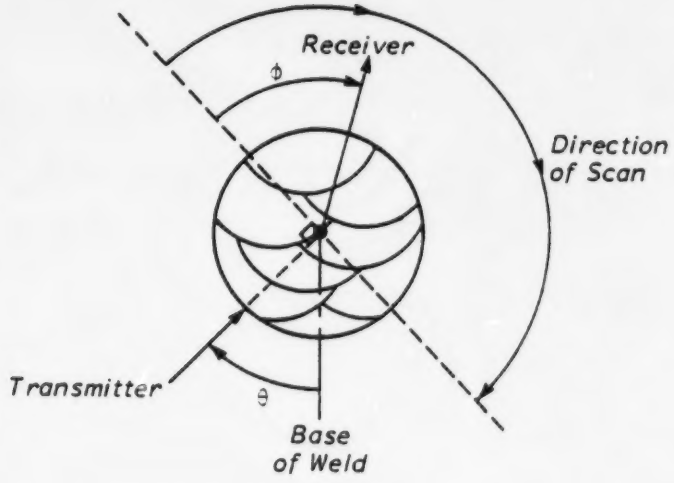

θ Cylinder Orientation Angle
Φ Receiver Angle

FIGURE 7
REFERENCE NOTATION FOR PLOTS (AFTER /19/)

FIGURE 8 : Variation of Skew Angle With the Orientation of the Cylinder

a) MILD STEEL

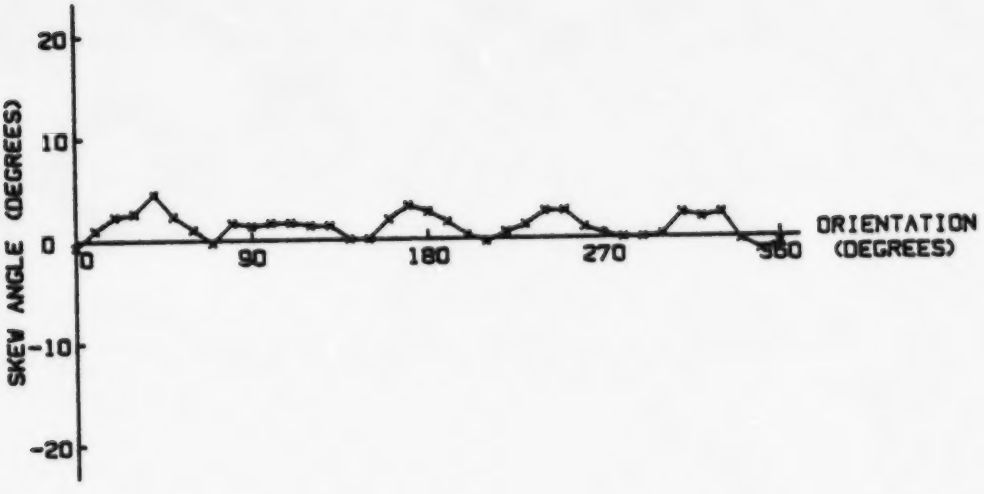

b) MILD STEEL WELD

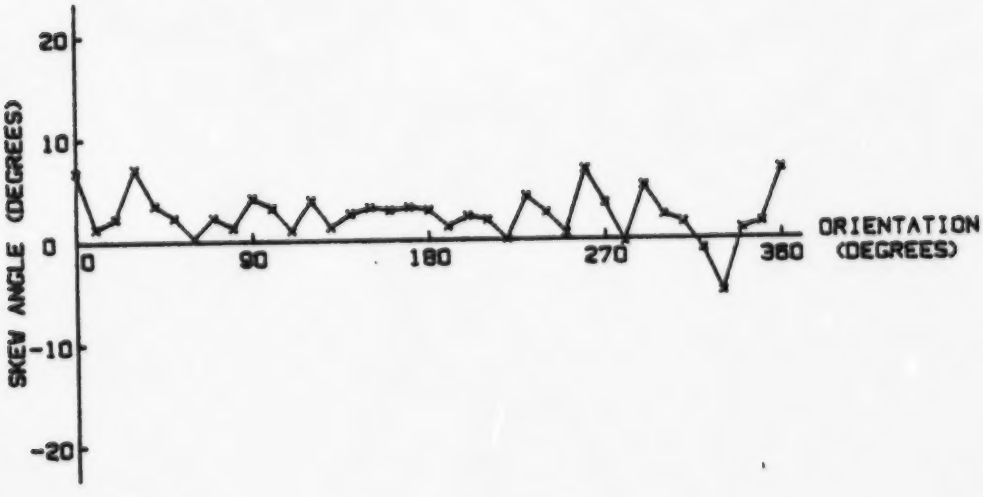

FIGURE 8 (Continued)

c) STAINLESS STEEL

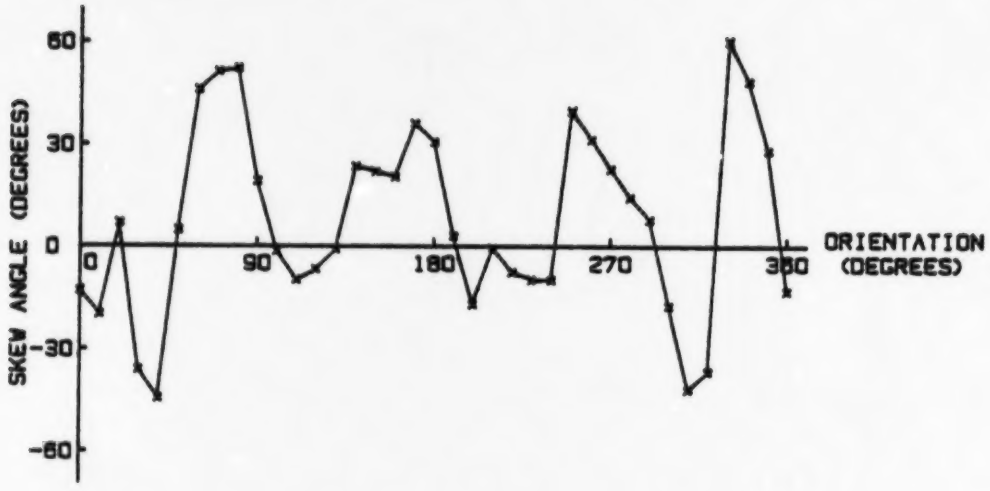

d) TITANIUM GR. 2

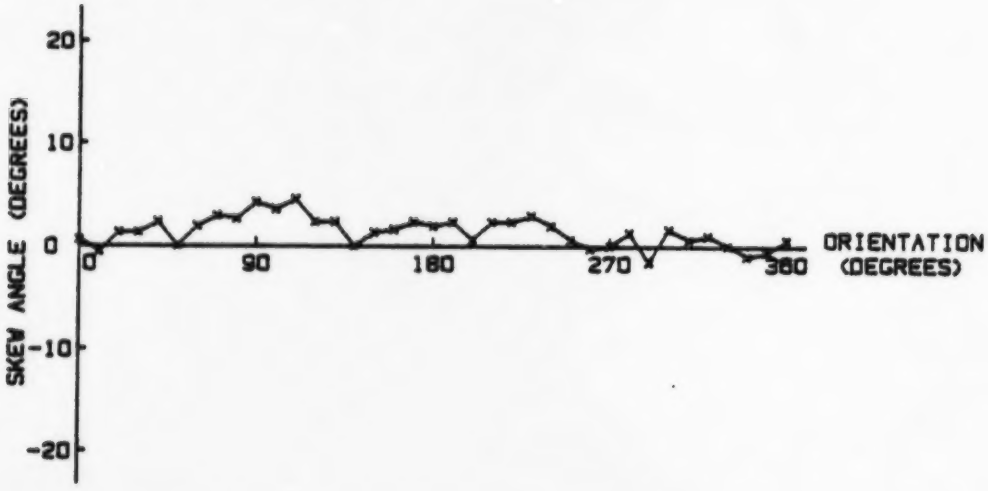

FIGURE 8 (Continued)

e) TITANIUM GR. 12 LT

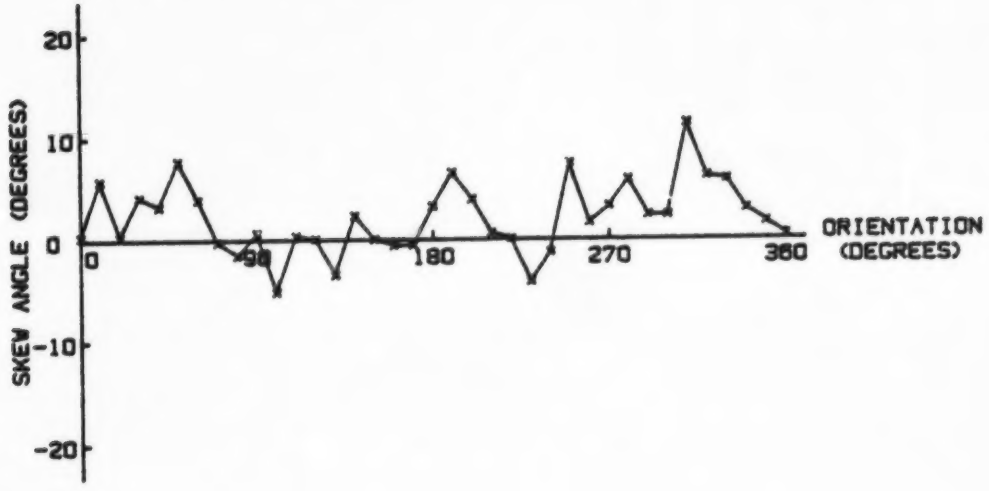

f) TITANIUM GR. 12 HT

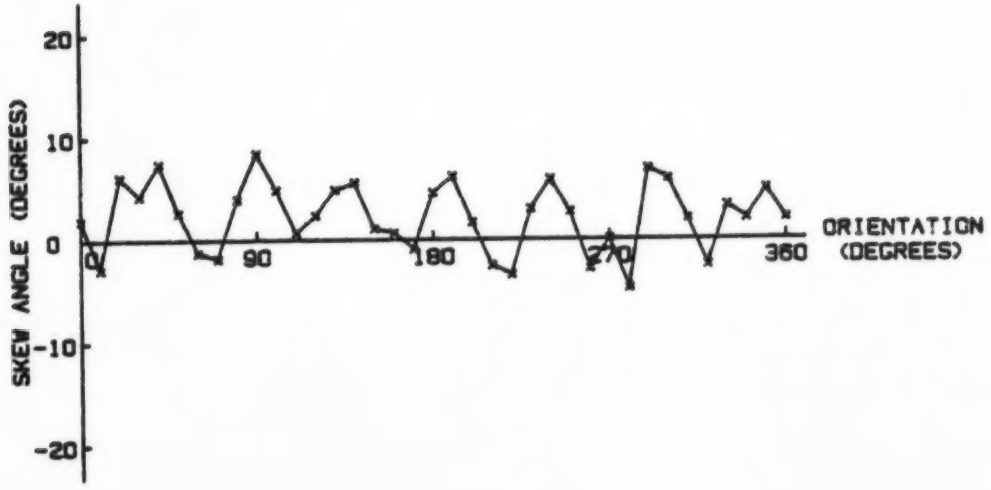

FIGURE 8 (Continued)

g) COPPER LT

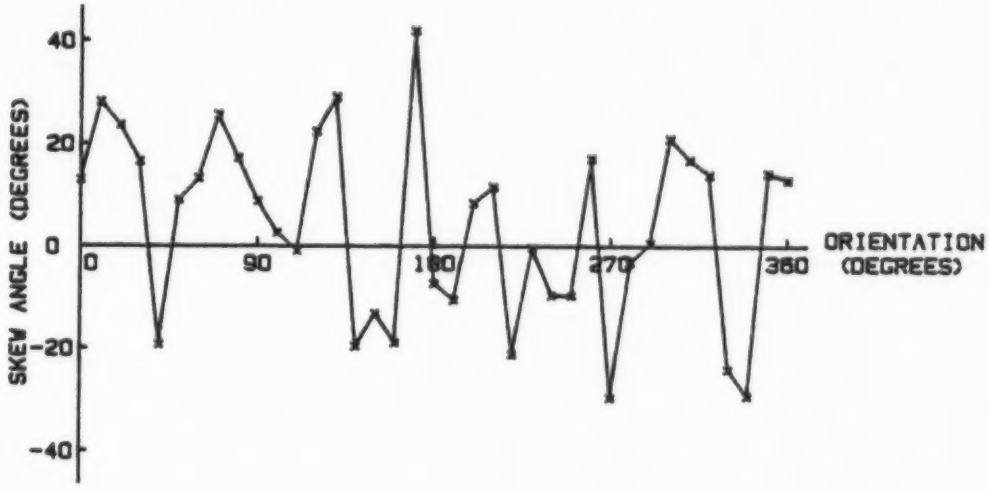

h) COPPER HT

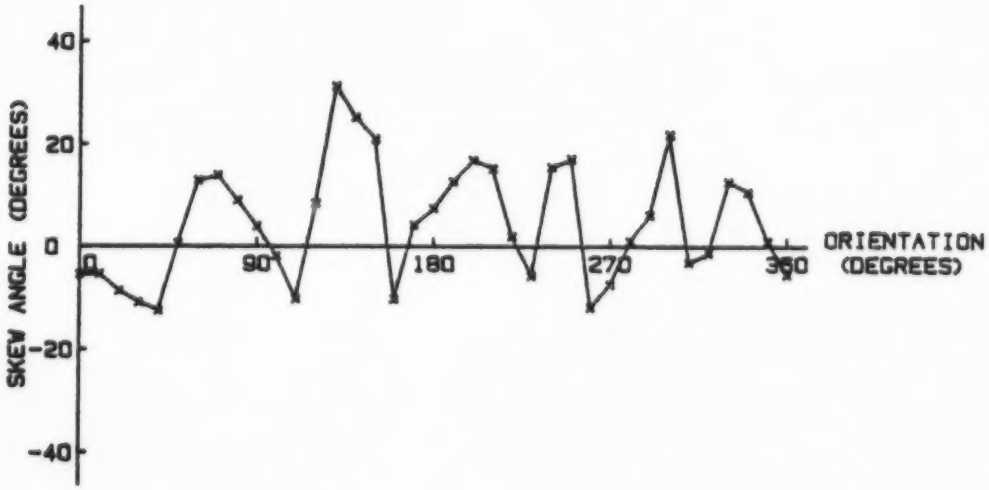

165768 RD

FIGURE 8 (Continued)

i) INCONEL 625 LT

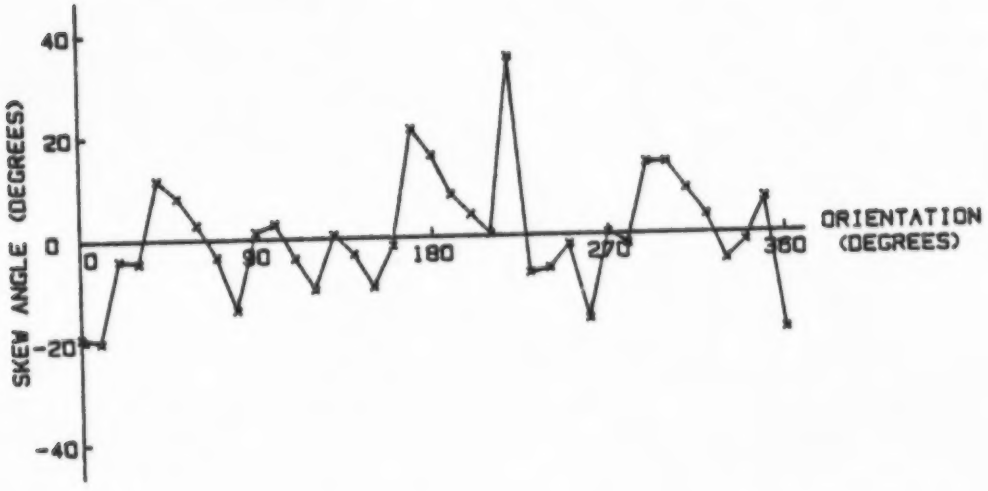

j) INCONEL 625 HT

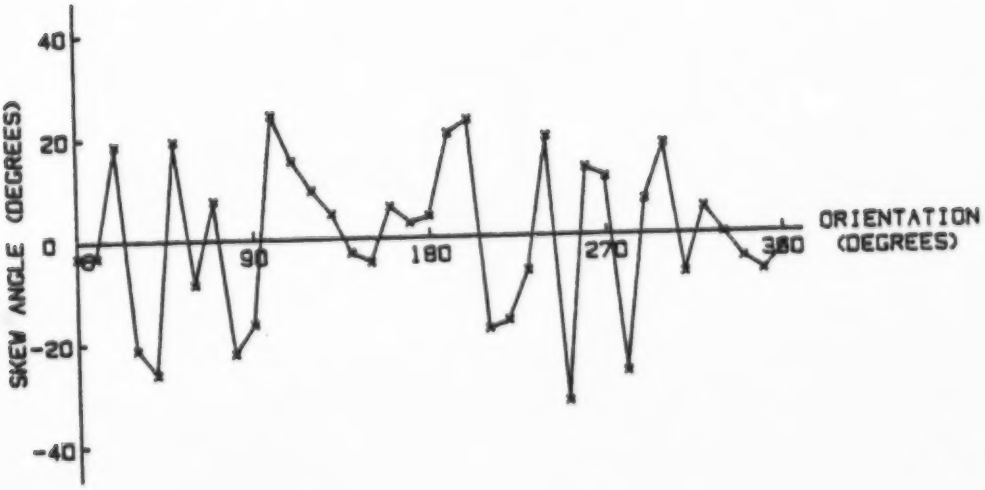

FIGURE 8 (Continued)

k) HASTELLOY C-276 LT

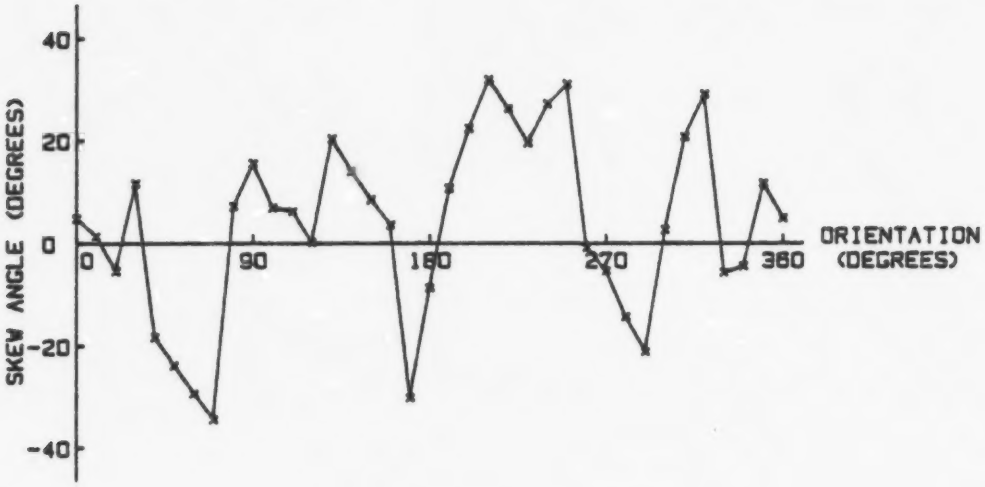

l) HASTELLOY C-276 HT

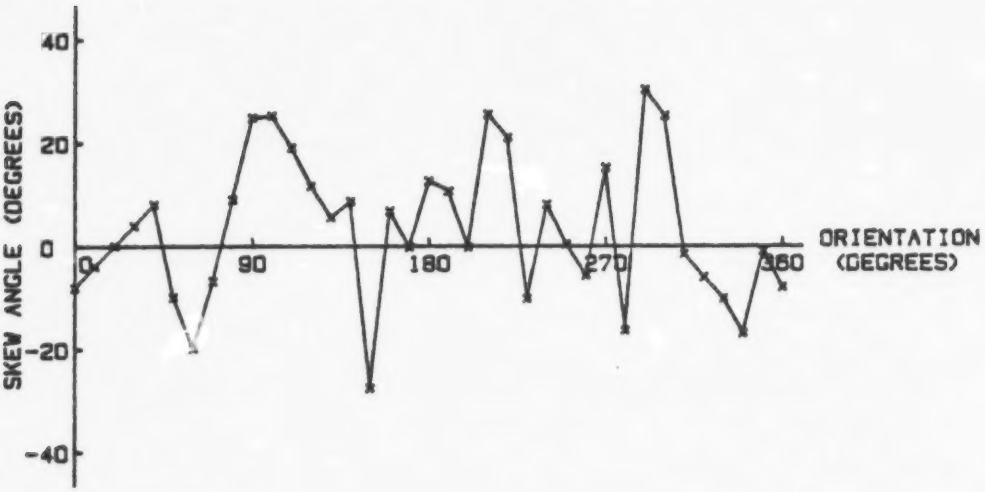

165770 RD